4 RESULTS

4.1 TraG-like proteins contain two conserved domains that probably form a nucleotide binding pocket

Sequence comparison of 19 representative TraG-like proteins of conjugative DNA transfer systems (like RP4, R388, F, Ti and pKM101 plasmids) and of other Type IV secretion systems involved in pathogenicity (*H. pylori*, *Wolbachia* sp. and *Rickettsia prowazeckii*) shows that TraG-like proteins contain two conserved domains (domains 1 and 2, Figure 4.2). Within these two domains, five motifs containing highly conserved residues were identified (motifs I - V, Figure 4.2). Motifs I and II resemble the Walker A and B motifs of nucleotide-binding proteins, as originally defined by Walker *et al.* (105). These motifs form a functional nucleotide binding pocket and are conserved in nucleotide hydrolases (NTPases) and ABC transporters (85, 85). Previous studies identified motifs I and II as essential motifs for transfer activity. K187T (motif I) and D448N (motif II) mutations in RP4 TraG, as well as K136T and K152A (motif I) mutations in R388 TrwB and Ti VirD4, respectively, resulted in transfer defective phenotypes (4, 48, 64). The recently solved crystal structure of truncated TrwB (TrwBΔN70), provided evidence for the existence of the proposed nucleotide binding pocket (Figure 4.1) (31).

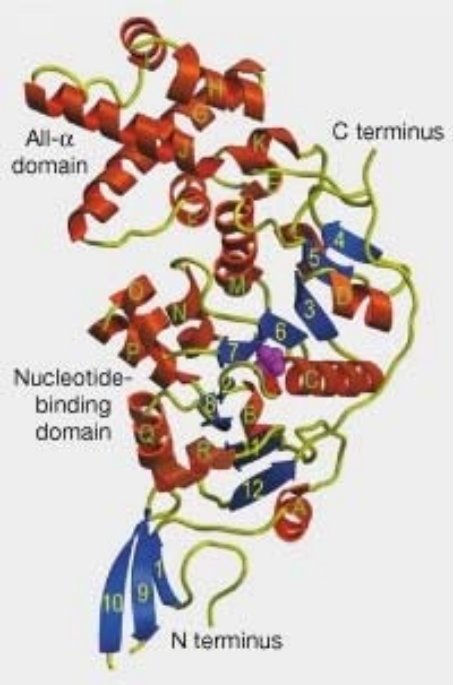

Figure 4.1. Structure of a TrwBΔN70 protomer. The ribbon diagram shows α-helices (in red colour, labelled A-R) and β-strands (in blue colour, numbered 1-12). A sulfate ion (labelled in magenta) occupies the nucleotide binding pocket. Protein domains and positions of the N- and C-termini of the protein are indicated. [Taken from Gomis-Rüth *et al.* (31)]

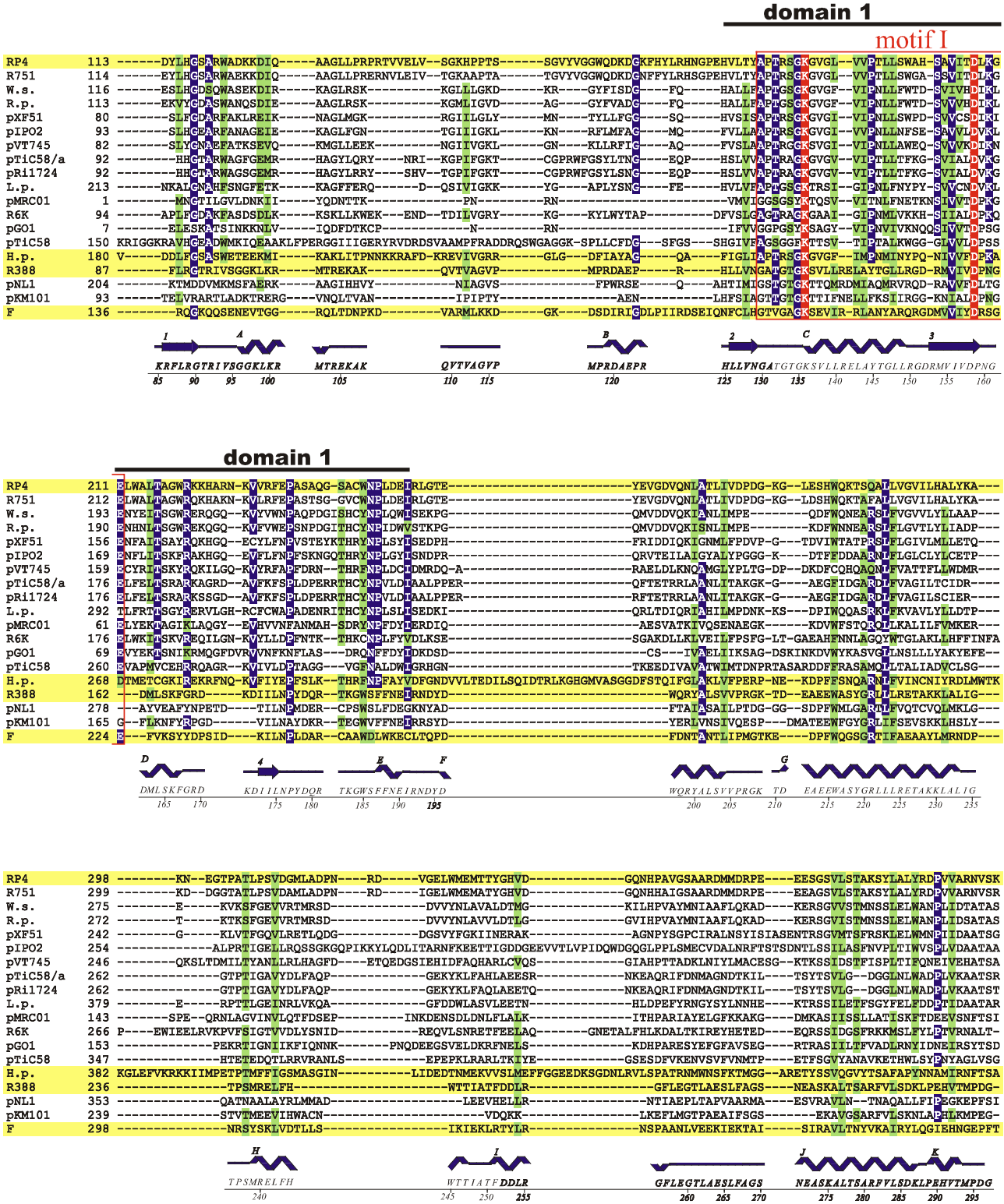
domain 1
motif I
RP4 113 ------DYLHGSARWADKKDIQ-----AAGLLPRPRTVVELV--SGKHPPTS------SGVYVGGWQDKDGKFHYLRHNGPEHVLTYAPTRSGKGVGL--VVPTLLSWAH-SAVITDLKG
R751 114 ------EYLHGSARWAEKKDIQ-----AAGLLPRERNVLEIV--TGKAAPTA------TGVYVGGWQDKDGNFFYLRHSGPEHVLTYAPTRSGKGVGL--VVPTLLSWGA-SSVITDLKG
W.s. 116 ------ESLHGDSQWASEKDIR-----KAGLRSK----------KGLLLGKD------KR----GYFISDGKGF--FQ-----HALLFAPTGSGKGVGF--VIPNLLFWTD-SVVEDIKL
R.p. 113 ------EKVYGDASWANQSDIE-----AAGLRSK----------KGMLIGVD------AG----GYFVADGKGF--FQ-----HALLFAPTGSGKGVGF--VIPNLLFWTD-SVVEDIKL
pXF51 80 -------SLFGDARFAKLREIK-----NAGLMGK----------RGIILGLY------MN----TYLLFGGKGF--SQ-----HVSISAPTRSGKGVGI--VIPNLLSWPD-SVVCSDIKI
pIPO2 93 -------SLHGDARFANAGEIE-----KAGLFGN----------TGIIIGKL------KN----RFLMFAGKGF--MQ-----FVLLAAPTRSGKGVGI--VVPNLLNFSE-SAVVLDVKL
pVT745 82 -------SLYGNAEFATKSEVQ-----KMGLLEEK---------NGIIVGKL------GN----KLLRFTGKGF--AQ-----FVSLAAPTRGGKSVGI--VIPNLLAWEQ-SVVVKDIKN
pTiC58/a 92 --------HHGTARWAGFGEMR-----HAGYLQRY----NRI--KGPIFGKT------CGPRWFGSYLTNGKGF--EQP----HSLVVAPTRAGKGVGV--VIPTLLTFKG-SVIALDVKG
pRi1724 92 --------HHGTARWAGSGEMR-----HAGYLRRY----SHV--TGPIFGKT------CGPRWFGSYLSNGKGF--EQP----HSLVVAPTRAGKGVGV--VIPTLLTFKG-SVIALDVKG
L.p. 213 ------NKALGNAHFSNGFETK-----KAGFFERQ------D--QSIVIGKK------YG----APLYSNGKGF--FE-----HVLVFAPTSGGKTRSI--GIPNLFNYPY-SVVCNDVKL
pMRC01 1 --------MNGTILGVLDNKII-----YQDNTTK----------PN---------RN----------------------VMVIGGSGSYKTQSV--VITNLFNETKNSIVVTDPKG
R6K 94 ------APLFGDAKFASDSDLK-----KSKLLKWEK---END--TDILVGRY------KG----KYLWYTAP---------DFVSLGATRAGKGAAI--GIPNMLVKKH-SIIALDPKQ
pGO1 7 -------ELESKATSINKKNLV-----IQDFDTKCP----------N---------RN----------------------IFVVGGPGSYKSAGY--VIPNVIVKNQQSIVVTDPSG
pTiC58 150 KRIGGKRAVHGPADWMKIQEAAKLFPERGGIIIGERYRVDRDSVAAMPFRADDRQSWGAGGK-SPLLCFDG---SFGS---SHGIVFAGSGGFKTTSV--TIPTALKWGG-GLVVLDPSS
H.p. 180 V------DDLFGSASWETEEKMI-----KAKLITPNNKKRAFD-KREVIVGRR------GLG---DFIAYAGKGF--QA----FIGLIAPTRSGKGVGF--IMPNMINYPQ-NIVVFDPKA
R388 87 -------FLRGTRIVSGGKLKR-----MTREKAK----------QVTVAGVP----------MPRDAEPR-----R-----HLLVNGATGTGKSVLLRELAYTGLLRGD-RMVIVDPNG
pNL1 204 -------KTMDDVMKMSFAERK-----AAGIHHVY----------NIAGVS----------FPWRSE-----Q----AHTIMIGSTGTGKTTQMRDMIAQMRVRQD-RAVVFDLTG
pKM101 93 ------TELVRARTLADKTRERG----VNQLTVAN----------IPIPTY----------AEN---------LHFSIAGTTGTGKTTIFNELLFKSIRGG-KNIAIDPNG
F 136 --------RQGKQQSENEVTGG-----RQLTDNPKD--------VARMLKKD------GK----DSDIRIGDLPIIRDSEIQNFCLHGTVGAGKSEVIR-RLANYARQRGDMVVIYDRSG
A
B
C
KRFLRGTRIVSGGKLKR
MTREKAK
QVTVAGVP
MPRDAEPR
HLLVNGATGTGKSVLLRELAYTGLLRGDRMVIVDPNG
85 90 95 100 105 110 115 120 125 130 135 140 145 150 155 160
domain 1
RP4 211 ELWALTAGWRKKHARN-KVVRFEPASAQG-SACWNPLDPIRLGTE----------YEVGDVQNLATLIVDPDG-KG--LESHWQKTSQALLVGVILHALYKA---
R751 212 ELWALTAGWRQKHAKN-KVLRFEPASTSG-GVCWNPLDPIRLGTE----------YEVGDVQNLATLIVDPDG-KG--LDSHWQKTAFALLVGVILHALYKA---
W.s. 193 ENYELTSGWRERQGQ--KVYVWNPAQPDGISHCYNPLQWISEKPG----------QMVDDVQKIANLIMPE--------QDFWQNEARSLFVGVVLYLLAAP---
R.p. 190 ENHNLTSGWREKQGQ--KVFVWEPSNPDGITHCYNPIDWVSTKPG----------QMVDDVQKISNLIMPE--------KDFWNNEARSLFLGVTLYLIADP---
pXF51 156 ENFALTSAYRQKHGQ--ECYLFNPVSTEYKTHRYNPLSYISEDPH----------FRIDDIQKIGNMLFPDVP-G---TDVIWTATPRSLFLGIVLMLLETQ---
pIPO2 169 ENFLLTSKFRAKHGQ--EVFLFNPFSKNGQTHRYNPLGYISNDPR----------QRVTEILAIGYALYPGGG-K----DTFFDDAARNLFLGLCLYLCETP---
pVT745 159 ECYRLTSKYRQKILGQ-KVYRFAPFDRN--THRFNPLDCIDMRDQ-A----------RAELDLKNQAMGLYPLTG-DP--DKDFCQHQAQNLFVATTFLLWDMR---
pTiC58/a 176 ELFELTSRARKAGRD--AVFKFSPLDPERRTHCYNPVLDIAALPPER----------QFTETRRLAANLITAKGK-G----AEGFIDGARDLFVAGILTCIDR-----
pRi1724 176 ELFELTSRARKSSGD--AVFKFSPLDPERRTHCYNPVLDIAALPPER----------RFTETRRLAANLITAKGK-G----AEGFIDGARDLFVAGILSCIER-----
L.p. 292 TLFRTTSGYRERVLGH-RCFCWAPADENRITHCYNPLSLISEDKI----------QRLTDIQRTAHILMPDNK-KS---DPIWQQASRKLFKVALYLLDTP---
pMRC01 61 ELYEKTAGIKLAQGY--EVHVVNFANMAH-SDRYNPFDYIERDIQ----------AESVATKIVQSENAEGK------KDVWFSTQRQLLKALILFVMKER---
R6K 176 ELWKLTSKVREQILGN-KVYLLDPFNTK--THKCNPLFYVDLKSE----------SGAKDLLKLVEILFPSFG-LT-GAEAHFNNLAGQYWTGLAKLLHFFINFA
pGO1 69 EVYEKTSNIKRMQGFDVRVVNFKNFLAS---DRQNFFDYIDKDSD----------CS---IVAELIIKSAG-DSKINKDVWYKASVGLLNSLLLYAKYEFE--
pTiC58 260 EVAPMVCEHRRQAGR--KVIVLDPTAGG---VGFNALDWIGRHGN----------TKEEDIAVATWIMTDNPRTASARDDFFRASAMQLLTALIADVCLSG---
H.p. 268 DTMETCGKIREKRFNQ-KVFIYEPFSLK--THRFNPFAYVDFGNDVVLTEDILSQIDTRLKGHGMVASGGDFSTQIFGLAKLVFPERP-NE--KDPFFSNQARNLFVINCNIYRDLMWTK
R388 162 ---DMLSKFGRD-----KDIILNPYDQR--TKGWSFFNPIRNDYD----------WQRYALSVVPRGK-TD--EAEEWASYGRLLLRETAKKLALIG---
pNL1 278 ---AYVEAFYNPETD----TILNPMDER--CPSWSLFDEGKNYAD----------FTATASAILPTDG-GG--SDPFWMLGARNLFVQTCVQLMKLG---
pKM101 165 G--FLKNFYRPGD------VILNAYDKR--TEGWVFFNEIRRSYD----------YERLVNSIVQESP---DMATEEWFGYGRLIFSEVSKKLHSLY---
F 224 E---FVKSYYDPSID----KILNPLDAR--CAAWDLWKECLTQPD----------FDNTANTLIPMGTKE----DPFWQGSGRTIFAEAAYLMRNDP---
D
4
E
F
G
DMLSKFGRD
KDIILNPYDQR
TKGWSFFNEIRNDYD
WQRYALSVVPRGK
TD
EAEEWASYGRLLLRETAKKLALIG
165 170 175 180 185 190 195 200 205 210 215 220 225 230 235
RP4 298 --------KN--EGTPATLPSVDGMLADPN----RD-----VGELWMEMTTYGHVD----------GQNHPAVGSAARDMMDRPE----EESGSVLSTAKSYLALYRDPVVARNVSK
R751 299 --------KD--DGGTATLPSVDAMLADPN----RD-----IGELWMEMATYGHVD----------GQNHHAIGSAARDMMDRPE----EEAGSVLSTAKSYLALYRDPVVARNVSR
W.s. 275 --------E-----KVKSFGEVVRTMRSD----------DVVYNLAVALDTMG----------KILHPVAYMNIAAFLQKAD----KERSGVVSTMNSSLELWANPLIDTATAS
R.p. 272 --------T-----KTKSFGEVVRTMRSD----------DVVYNLAVVLDTLG----------GVIHPVAYMNIAAFLQKAD----KERSGVISTMNSSLELWANPLIDSATAS
pXF51 242 --------G-----KLVTFGQVLRETLQDG----------DGSVYFGKIINERAK----------AGNPYSGPCIRALNSYISIASENTRSGVMTSFRSKLELWMNPIIDAATSG
pIPO2 254 ------------ALPRTIGELLRQSSGKGQPIKKYLQDLITARNFKEETTIGDDGEEVVTLVPIDQWDGQGLPPLSMECVDALNRFTSTSDNTLSSILASFNVPLTIWVSPLVDAATAA
pVT745 246 --------QKSLTDMILTYANLLRLHAGFD----ETQEDGSIEHIDFAQHARLCVQS----------GIAHPTTADKLNIYLMACESG--KTKSSIDSTFISPLTIFQNEIVEHATSA
pTiC58/a 262 --------------GTPTIGAVYDLFAQP----------GEKYKLFAHLAEESR----------NKEAQRIFDNMAGNDTKIL----TSYTSVLG--DGGLNLWADPLVKAATSR
pRi1724 262 --------------GTPTIGAVYDLFAQP----------GEKYKLFAQLAEETQ----------NKEAQRIFDNMAGNDTKIL----TSYTSVLG--DGGLNLWADPLVKAATST
L.p. 379 --------E-----RPTTLGEINRLVKQA----------GFDDWLASVLEETN----------HLDPEFYRNGYSYLNNHE----KTRSSILETFSGYFELFDDPTIDAATAR
pMRC01 143 -------SPE--QRNLAGVINVLQTFDSEP---------INKDENSDLDNLFLALK----------ITHPARIAYELGFKKAKG----DMKASIISSLLATISKFTDEEVSNFTSI
R6K 266 P----EWIEELRVKPVFSIGTVVDLYSNID----------REQVLSNRETFEELAQ-------GNETALFHLKDALTKIREYHETED----EQRSSIDGSFRKKMSLFYLPTVRNALT-
pGO1 153 -------------PEKRTIGNIIKFIQNNK-------PNQDEEGSVELDKRFNELS----------KDHPARESYEFGFAVSEG----RTRASIILTFVADLRNYIDNEIRSYTSD
pTiC58 347 -------------HTETEDQTLRRVRANLS----------EPEPKLRARLTKIYE----------GSESDFVKENVSVFVNMTP----ETFSGVYANAVKETHWLSYPNYAGLVSG
H.p. 382 KGLEFVKRKKIIMPETPTMFFIGSMASGIN----------LIDEDTNMEKVVSLMEFFGGEEDKSGDNLRVLSPATRNMWNSFKTMGG--ARETYSSVQGVYTSAFAPYNNAMIRNFTSA
R388 236 ---------------TPSMRELFH----------WTTIATFDDLR----------GFLEGTLAESLFAGS----NEASKALTSARFVLSDKLPEHVTMPDG-
pNL1 353 -------------QATNAALAYRLMMAD----------LEEVHELLR----------NTIAEPLTAPVAARMA----ESVRAVLN--TNAQALLFIPEGKEPFSI
pKM101 239 -------------STVTMEEVIHWACN----------VDQKK----------LKEFLMGTPAEAIFSGS-------EKAVGSARFVLSKNLAPHLKMPEG-
F 298 ---------------NRSYSKLVDTLLS----------IKIEKLRTYLR----------NSPAANLVEEKIEKTAI-----SIRAVLTNYVKAIRYLQGIEHNGEPFT
H
I
J
K
TPSMRELFH
WTTIATFDDLR
GFLEGTLAESLFAGS
NEASKALTSARFVLSDKLPEHVTMPDG
240 245 250 255 260 265 270 275 280 285 290 295

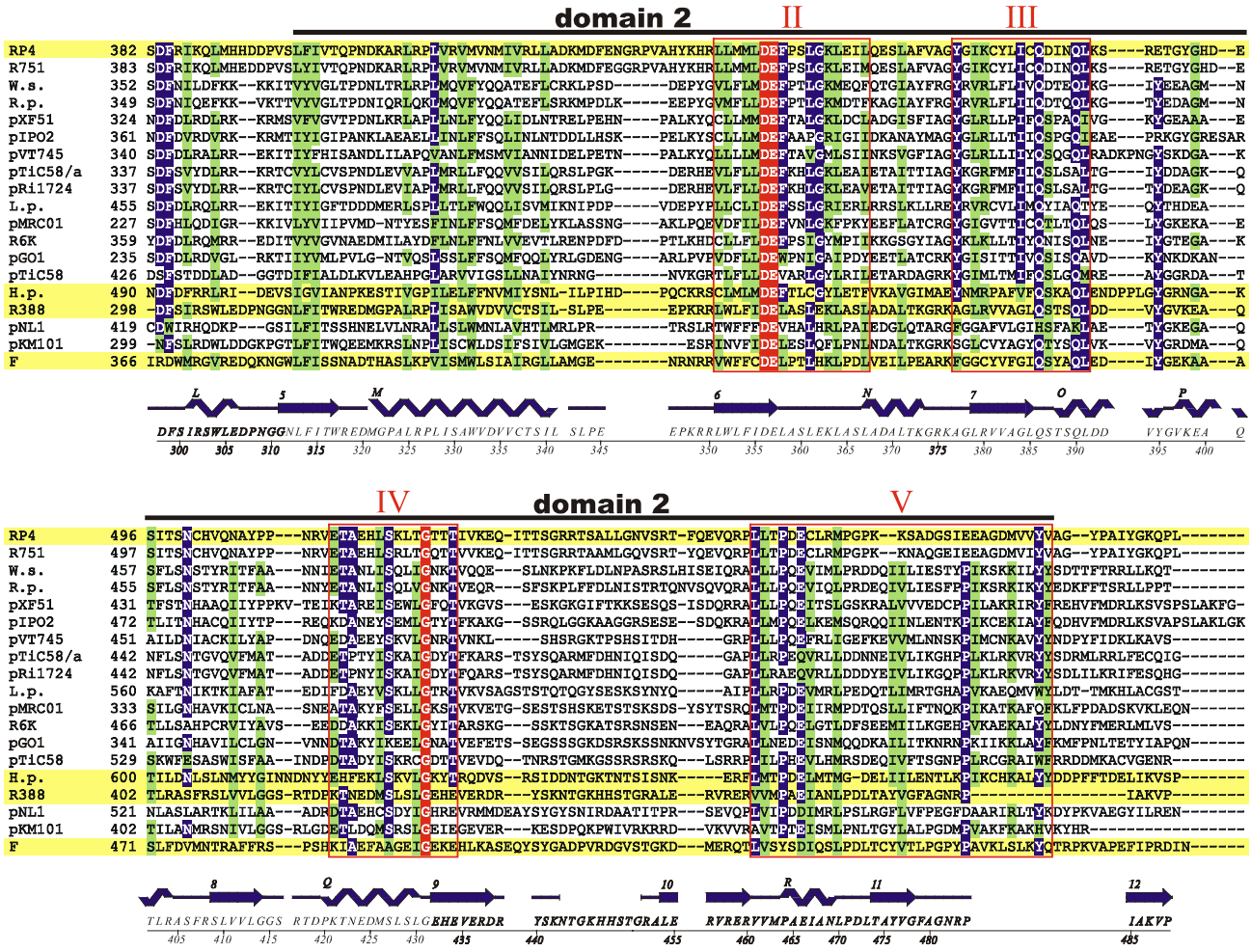

Figure 4.2. TraG-like proteins of conjugative transfer systems and of other type IV secretion systems contain two conserved domains probably forming a functional nucleotide binding domain (NBD). Amino acid sequences of 19 different TraG-like proteins are aligned. Domains 1 and 2 are delimited by black bars drawn above the sequences. Conserved motifs I-V inside these domains are framed in red. Peptide sequences of the four proteins that were studied in the present work are highlighted in yellow. The structure of R388 TrwBΔN70 as a ribbon diagram is superimposed to the sequence alignment. α-helices (A-R) and β-strands (1-12) are labelled as in Figure 4.1. The origin of each protein (plasmid or chromosome) is indicated to the left. Amino acid positions that are conserved throughout are highlighted in red; identical residues present in at least 68% of the sequences are marked by blue background; green shading indicates similar residues in at least 68% of the sequences. Accession numbers are as follows: TraG (RP4), S22999; TraG (R751), S22992; VirD4 (*Wolbachia* sp. strain wKueYO [W.s.]), BAA97443; VirD4 (*Rickettsia prowazeckii* [R.p.]), H71684; VirD4 (pXF51), NP_061672; TraN (pIPO2), AJ297913); MagB12 (pVT745), NP_067572; VirD4 (pTiC58/a), P18594; VirD4 (pRi1724), NP_066751; LvhD4 (*Legionella pneumophila* [L.p.]), CAB60062; TrsK (pMRC01), NP_047302; TaxB (R6K), CAA71845; TrsK (pGO1), C56976; TraG (pTiC58), Q44346; HP0524 (*H. pylori* [H.p.]), NP_207320; TrwB (R388), S43877; TraD (pNL1), NP_049138; TraJ (pKM101), T30861; TraD (F), NP_061481.

Walker A consensus motif (G/AxxxxGKS/T), the phosphate-binding loop (P-loop), is perfectly conserved in some of the TraG-like proteins (like R388 TrwB and F TraD) but contains a substitution in many of the sequences (like RP4 TraG and Ti VirD4), where the sequence is AxxxxGKG (the substitution is underlined). This sequence however exactly matches the P-loop sequence of adenylate kinases (82) and may therefore be considered as a functional P-loop motif.

The structural information contained in the crystal structure of TrwBΔN70 was superimposed to the sequence alignment in Figure 4.2. This structure-sequence alignment enabled the identification of structural features that are supposedly conserved among TraG-like proteins. The conserved domains 1 and 2 contain the nucleotide binding domain (NBD) of R388 TrwB, including β-strands 2-11 and α-helices C-E and M-R. The nucleotide binding pocket is formed by structural elements that are comprised in the conserved motifs I, II and III. Motif I consists of the P-loop, followed by helix C and strand 3. Separated by 190 (TrwB) to 277 (HP0524) residues, are following strand 6 of motif II and strand 7 of motif III that form a β-sheet with strand 3. A second loop structure, located between helix R and strand 11 (motif V) comes to close proximity to the nucleotide binding pocket. Motif IV contains helix Q, followed by a short loop and the beginning of β-sheet 9. These structures are located at the inside of the channel of TrwBΔN70 hexamers, close to the putative transmembrane passage. Motif IV may thus harbor functions essential for recognition and/or gating of a substrate that may possibly be secreted through the pore and into the periplasm.

The variable region between motifs I and II is exclusively composed of α-helices forming a separate domain in the case of TrwB (all-α-domain, Figure 4.1), and it may be assumed that similar structures are formed in other TraG-like proteins. The all-α-domain is possibly a strictly structural feature that does not require the presence of specific residues. Likewise, the C-terminus is less conserved and varies strongly in its length. The N-terminus is weakly conserved but is required for anchoring the protein to the inner membrane and for multimerization, as will be shown (4.2, 4.5 and 4.8.2). Further indications for the role of some of the domains or motifs of TraG-like proteins were gained from mutational analysis of RP4 TraG (4.3).

4.2 The topology of integral membrane protein TraG resembles the topology of F TraD and Ti VirD4

TraG contains two significant clusters of hydrophobic residues (from Val23 to Leu66 and from Ala83 to Val104), consistent with the protein potentially possessing two or three transmembrane domains. The membrane topology of TraG was analyzed by a method allowing positive identification of periplasmic domains by analysis of in-frame insertion derivatives. This method has been used previously to confirm the membrane topologies of LacY and of the serine chemoreceptor (Tsr) and to determine the membrane topology of F TraD (53).

20 in-frame insertion mutants containing 31-residue insertion sequences were created (TraGi31 mutants, Table 4.1). Insertion mutagenesis was performed by transposition with transposons Tn*lacZ/in* or Tn*phoA/in* and subsequent deletion of most of the inserted sequence (Figure 3.3, page 24).

Table 4.1. Transfer activity and trypsin sensitivity of TraG insertion mutants.

traG Plasmid	TraG protein	Transconjugants/Donor	Transfer activity[a]	Trypsin sensitivity[b]
pSK470	TraG	40	++	-
pMS119	/	$<10^{-6}$	-	/
p*traG::i31*Ser30	TraGiS30	$4\cdot10^{-4}$	+/-	ND
p*traG::i31*Gly32	TraGiG32	$2\cdot10^{-4}$	+/-	ND
p*traG::i31*Gly53	TraGiG53	10	++	+
p*traG::i31*Gly74	TraGiG74	$2\cdot10^{-2}$	+	+
p*traG::i31*Gly87	TraGiG87	$8\cdot10^{-5}$	+/-	+
p*traG::i31*Ala119	TraGiA119	$1\cdot10^{-3}$	+	-
p*traG::i31*Glu141	TraGiE141	3	++	ND
p*traG::i31*Ser153	TraGiS153	2	++	-
p*traG::i31*Glu175	TraGiE175	$4\cdot10^{-3}$	+	ND
p*traG::i31*Asn243	TraGiN243	$7\cdot10^{-1}$	++	-
p*traG::i31*Glu255	TraGiE255	$4\cdot10^{-2}$	+	ND
p*traG::i31*Ala344	TraGiA344	$5\cdot10^{-3}$	+	-
p*traG::i31*Ser397	TraGiS397	74	++	-
p*traG::i31*Gly455	TraGiG455	$<10^{-6}$	-	ND
p*traG::i31*Lys473	TraGiK473	$<10^{-6}$	-	ND
p*traG::i31*Asn482	TraGiN482	$6\cdot10^{-5}$	+/-	-
p*traG::i31*Glu516	TraGiE516	$2\cdot10^{-4}$	+/-	-
p*traG::i31*His517	TraGiH517	$<10^{-6}$	-	ND
p*traG::i31*Glu552	TraGiE552	$<10^{-6}$	-	ND
p*traG::i31*Val612	TraGiV612	61	++	-

[a] transfer activity is defined as positive (++) with wild type TraG (pSK470) or negative (-) without TraG (pMS119) expressed from the complementary plasmid in the mating experiment. + and +/- indicate intermediate and weak activities, respectively.
[b] ND, not determined

The 31-codon in-frame insertion was identifiable in the resulting TraGi31 proteins by immunoblot analysis with specific antibodies. Additionally, the inserted sequence was detectable by proteolysis, since it contained a trypsin cleavage site. This trypsin-sensitivity was utilized to study the membrane topology of TraGi31 mutants by a whole-cell trypsinization assay of spheroplasted cells expressing the TraGi31 proteins. In spheroplasted cells, the periplasmic domains of TraG are exposed to proteases, whereas cytoplasmic domains are protected by the inner membrane. Periplasmic domains are usually trypsin-resistant, as is seen for many cytoplasmic membrane proteins with substantial periplasmic domains (like Tsr and TraD). However, when the 31-residue trypsin-sensitive insertion is exposed in periplasmic domains, the protein is cleavable by trypsin.

Trypsinization of spheroplasts expressing wild-type TraG confirmed that the periplasmic domain of TraG was trypsin-resistant. In contrast, TraGiG53, TraGiG74, and TraGiG87 were sensitive to trypsin (Figure 4.3). This observation suggests that the insertions at residues 53, 74, and 87 were translocated to the periplasmic space. The remaining TraGi31 proteins were trypsin-resistant, indicating that the insertions in these proteins were retained in the cytoplasm.

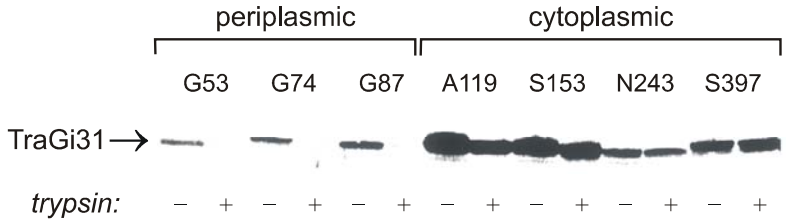

Figure 4.3. Trypsin sensitivity of TraG insertion mutants. Cells expressing TraG insertion mutants (TraGi31) were spheroplasted and treated with (+) or without (-) trypsin prior to immunoblot analysis. Antibodies directed against the trypsin sensitive insertion sequence were used for detection of the different mutant proteins (53).

Thus, TraG contains a single periplasmic domain spanning approximately from residue His44 to Gly87. Since insertions before and after that domain were trypsin-resistant, the N- and C-termini of TraG are likely to be localized to the cytoplasm. Two transmembrane sequences are most probably located at residues 23-43 and 88-104, separating both cytoplasmic domains from the periplasmic domain. The positive charge of the cytoplasmic N-terminus (residues 1 – 22, 7 positive charges), is supportive of the "positive-inside" rule for membrane proteins (104). This rule implicates that positively charged domains adjacent to membrane-spanning domains are likely to be located in the

cytoplasm. The proposed topology of TraG (represented in Figure 4.4) strongly resembles the topology determined for F TraD (53) and Ti VirD4 (22).

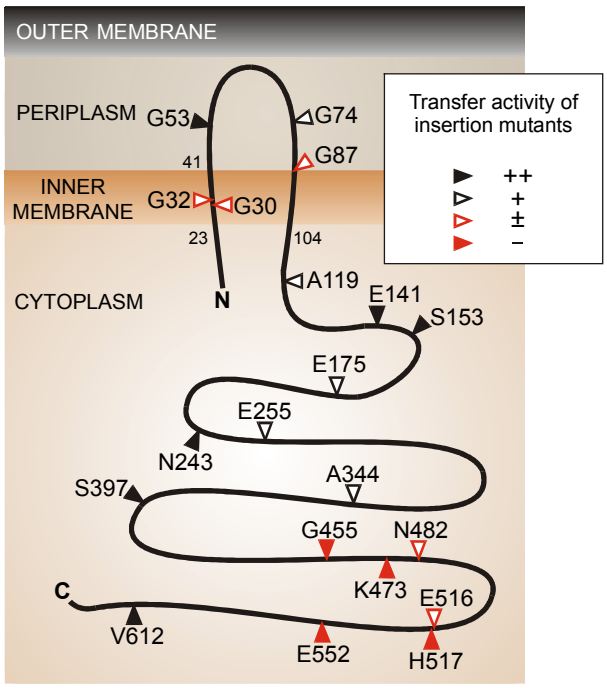

Figure 4.4. Proposed topology of RP4 TraG. In frame insertion mutants of TraG were generated for identification of periplasmic domains and for detection of non-permissible insertion sites. Arrowheads depict the insertion site; the last unaltered amino acid and its position are given. The transfer frequency of each mutant was determined in mating assays (Table 4.1).

4.3 Mutational analysis of TraG allowed the identification of functionally essential domains

The 20 insertion mutants of TraG that were generated for determination of the topology (TraGi31 mutants, Table 4.1) were also analyzed for their ability to support conjugative transfer. The different p*TraG::i31* plasmids were provided *in trans* for complementation of pDB127, a derivative of conjugative plasmid pDB126 lacking *traG* (Table 2.2). Among the 20 mutants tested, four insertions had a transfer defective phenotype and another five insertions conferred substantially decreased transfer frequencies (listed in Table 4.1 and indicated in red in Figure 4.4). Strikingly, all of the mutations leading to a complete loss of transfer activity are located inside domain 2 of TraG, downstream of motif II (Figure 4.2). Thus, in addition to motives I and II, the conserved motifs III-V play essential roles for TraG function in conjugative transfer. When applied to the structure-sequence alignment of TraG-like proteins (Figure 4.2), essential functions can be attributed to strands 7 and 10 and to helices O and Q, for these structures are likely to become disrupted by the 31-amino acid insertion. Moreover, insertion into the loop

following strand 6 substantially reduced transfer activity of TraG. The three remaining mutants severely affecting transfer activity are located inside or adjacent to the proposed transmembrane domains of TraG (residues 23 to 41 and 88 to 104). Insertion of the 31-amino acid sequence into a transmembrane sequence is likely to prevent the insertion of this domain into the membrane. It is therefore proposed that insertions at residues 30 and 32 (and perhaps 87) inhibit proper translocalization of the transmembrane domains of TraG into the inner membrane and that membrane association is critical for TraG activity.

In addition to the insertion mutants, His_6-fusion mutants His_6-TraG and TraG-His_6 (43) and deletion mutants TraGΔ1 and TraGΔ2, that were constructed for purification (4.4), were analyzed for conjugation activity. TraGΔ1 lacks the short cytoplasmic N-terminus and the first of two transmembrane domains of TraG. In TraGΔ2, the periplasmic domain and the second transmembrane domain of TraG are additionally removed (Figure 4.5, page 47). Both deletion derivatives, encoded by pGS006Δ1 and pGS006Δ2 (Table 2.2), were unable to restore transfer activity in complementation experiments with pDB127. Thus, the entire membrane anchor of TraG is required for transfer activity. In contrast, His_6-TraG and TraG-His_6 were as effective as wild-type TraG in complementing pDB127 (43, 87).

The set of TraG mutants analyzed in the present work broadens the previous knowledge on the functional relevance of different domains of TraG-like proteins. Apart from RP4 TraG, mutants of F TraD, R388 TrwB and Ti VirD4 have been analyzed in genetic complementation studies (48, 53, 64). A summary of the conjugative transfer activities of these mutant proteins, along with the activities of TraG mutants here determined is presented in the discussion section (chapter 5).

4.4 TraG-like proteins originating from conjugative transfer systems RP4, F and R388 and from the type IV secretion system of *H. pylori* were purified

To characterize the biochemical properties of TraG-like proteins, full-length proteins, deletion derivatives and point mutation derivatives of several representatives originating from different conjugation/secretion systems were purified (Table 4.2). The purification of hexahistidine (His_6) tagged derivatives of full-length TraG and TraD has been described previously (43, 87). Due to experimental difficulties encountered with the

restricted solubility of TraG and the presence of detergent in TraG preparations, derivatives of TraG with anticipated improved qualities were generated.

Table 4.2. Origin, name and modification of TraG-like proteins purified in this work.

Origin	Description	TraG-like protein	TraG-like protein derivative purified in this work
RP4	IncPα conjugative plasmid, broad host range, self-transfer and mobilizing capacity for IncQ plasmids, rigid pili	TraG	His_6-TraG His_6-TraGK187T His_6-TraGΔ2 His_6-TraGΔ2K187T
R388	IncW conjugative plasmid, broad host range, self-transfer and mobilizing capacity for IncQ plasmids, rigid pili	TrwB	His_6-TrwBΔ1
F	IncF conjugative plasmid, narrow host range, self-transfer and mobilizing capacity for ColE1 plasmids, flexible pili	TraD	His_6-TraD
H. pylori	Cancer associated genes (*cag*) of the pathogenicity island (PAI) encoding the pathogenicity-related type IV secretion system of *H. pylori*	HP0524	His_6-HP0524Δ1

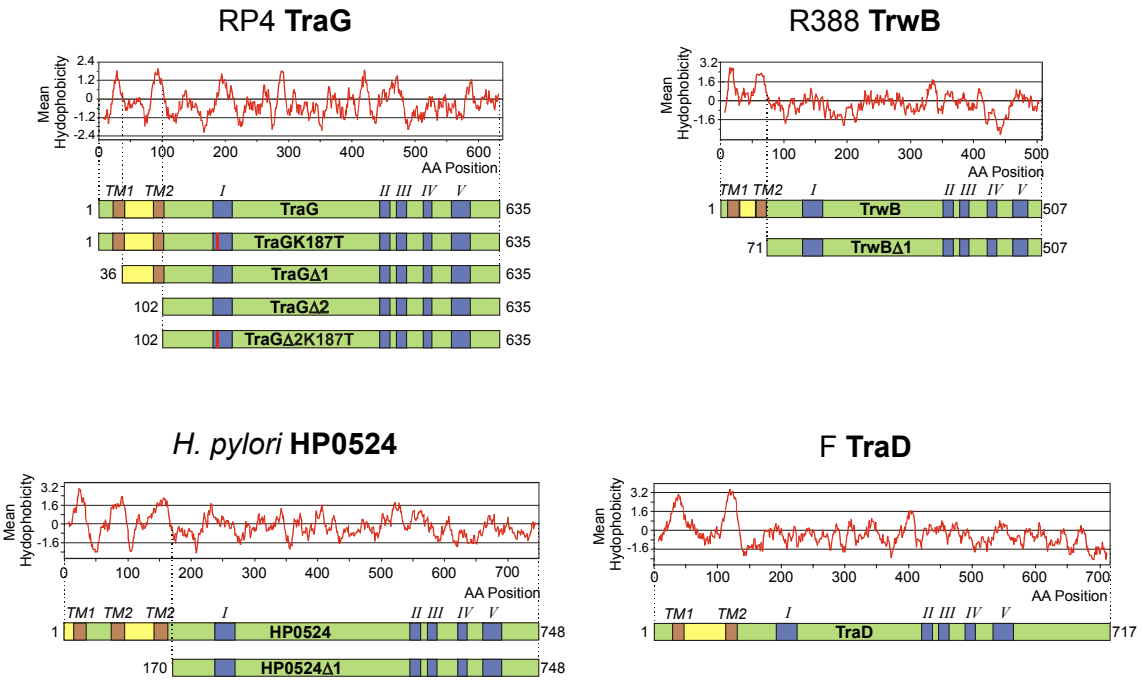

Figure 4.5. TraG-like proteins and derivatives purified in this work. The graphs show the calculated hydrophobicity profiles of TraG, TrwB, HP0524 and TraD. Amino acid (AA) positions are indicated. The proposed domain structures of the proteins and their derivatives are schematically represented. Cytoplasmic domains (green boxes), transmembrane segments (TM, brown boxes), periplasmic domains (yellow boxes) and conserved motifs (blue boxes, labeled I to V) are indicated. Vertical red bars represent the K187T mutation in the conserved Walker motif A of RP4 TraG.

Truncated (Δ) derivatives of TraG were designed for removal of the membrane anchor, which is located at the N-terminus of the protein (4.2). Moreover, point mutation

derivatives of TraG were purified that contain an amino acid substitution (K187T) in the proposed Walker box A (P-loop) motif of the nucleotide binding domain. The membrane topology of TrwB and of HP0524 was deduced from the calculated hydrophobicity profile of the proteins and by comparison to the sequences and hydrophobicity profiles of TraG and TraD with known topologies. Based on this prediction, truncated derivatives of TrwB and HP0524 that lack the putative transmembrane segments were generated. The proposed domain structures of TraG, TraD, TrwB and HP0524, along with the derivatives purified in this work, are shown in Figure 4.5.

4.4.1 Purification of RP4 TraG and TraGK187T

N-terminal modification with a hexahistidine (His_6) tag enabled purification of TraG and TraGK187T by affinity chromatography on nickel-nitrilotriacetic acid (Ni NTA). TraG was overproduced in *E. coli* cells harboring pFS241 (Table 2.2). Proteins from the crude cell extract were precipitated by addition of $(NH_4)_2SO_4$ (60% saturation) and were applied to Ni-NTA chromatography. Elution from the affinity matrix yielded a TraG preparation with a purity of 55% (Table 4.3). TraG migrates as a 71 kDa protein on SDS-polyacrylamide gels (Figure 4.7). Its identity was confirmed by N-terminal sequencing. The TraG preparation was further analyzed by Western blotting, using polyclonal antibodies against TraG (data not shown). The major impurity, a 59 kDa protein, was analyzed by N-terminal sequencing. It was identified to be a C-terminally truncated His_6-TraG derivative (43).

In analogy to TraG, TraGK187T was purified as a His_6-derivative, encoded by pFS241M (Table 2.2). Purification was performed following the same protocol as for TraG (see above), yielding a preparation of 49% purity (Table 4.3).

4.4.2 Purification of truncated RP4 TraG derivatives TraGΔ2 and TraGΔ2K187T

Plasmids encoding truncated TraG derivatives TraGΔ1 and TraGΔ2 (pGS006Δ1 and pGS006Δ2) were constructed by PCR with modified primers. The proteins were overproduced and assayed for solubility. Under native conditions, using mild non-ionic detergents Brij-58 or Triton X-100, TraGΔ1 remained insoluble. In contrast, native extraction of TraGΔ2 proved to be highly efficient. The solubility of TraGΔ2 was largely increased when compared to full-length TraG. The crude extract, containing

42% TraGΔ2, was purified by successive Ni-NTA affinity and phosphocellulose P11 chromatography, yielding a TraGΔ2 preparation of 85% purity (Table 4.3).

TraGΔ2K187T is a derivative of TraGΔ2 containing a mutation in the putative nucleotide binding signature (motif I). TraGΔ2K187T was purified from *E. coli* cells carrying pGS0011, following the same purification scheme as used for TraGΔ2. An SDS-PAGE that was run with the protein fractions collected during purification of TraGΔ2K187T is shown in Figure 4.6. Here, TraGΔ2 derivatives migrate as proteins with a size of 59 kDa.

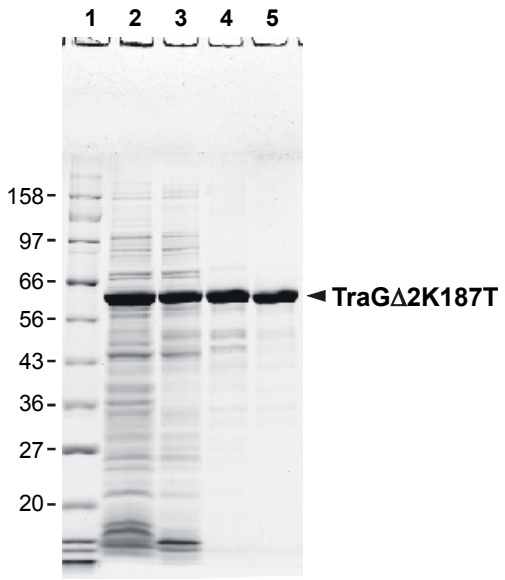

Figure 4.6. Truncated derivatives of RP4 TraG were purified in two steps. Coomassie-Blue-stained gel of samples collected during the purification of TraGΔ2K187T, resolved by SDS-PAGE. Lane 1, marker proteins (sizes in kDa are indicated). Lane 2, SDS complete cell extract (20 µg). Lanes 3-5, samples of native protein extracts: 3, fraction I (17 µg); 4, fraction II (9 µg); 5, fraction III (7 µg).

Table 4.3. Purification of TraG and TraG derivatives.

Protein	Fraction	Purification step	Total protein [mg]	Yield [%][a]	Purity [%][b]
TraG	I	Crude extract	1139	100	18
	II	Ni-NTA	87	23	55
TraGK187T	I	Crude extract	256	100	8.2
	II	Ni-NTA	7.8	18	49
TraGΔ2	I	Crude extract	645	100	42
	II	Ni-NTA	315	80	69
	III	Phosphocellulose P11	98	31	85
TraGΔ2K187T	I	Crude extract	753	100	30
	II	Ni-NTA	344	94	62
	III	Phosphocellulose P11	107	38	80

[a] Based upon TraG yield of fraction I
[b] Laser-densitometric evaluation of Coomassie-blue stained gels

4.4.3 Purification of F TraD

TraD was overproduced in *E. coli* cells harboring pSK410NH (Table 2.2). The protein was solubilized in a buffer containing 1% Triton X-100 as described previously (69). It was then purified by affinity chromatography on Ni-NTA, yielding a TraD preparation of only 42% purity but containing no major impurities (Table 4.4). On SDS-PAGE, TraD has a size of 81 kDa (Figure 4.7).

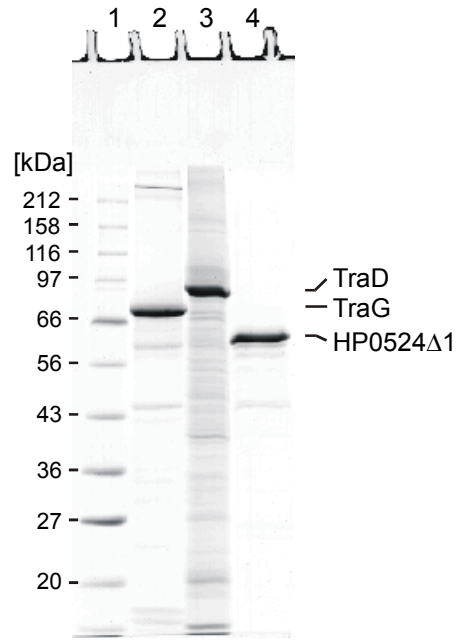

Figure 4.7. The full-length forms of TraG and TraD and a truncated derivative of HP0524 were purified. Samples of each protein (7 µg) were loaded to an SDS-15%-polyacryl-amide gel, resolved by electrophoresis and stained with Coomassie Blue. Lane 1, marker proteins (masses are given in kDa); lane 2, purified TraG (His_6-TraG); lane 3, purified TraD (His_6-TraD); lane 4, purified HP0524Δ1 (His_6-HP0524Δ1).

4.4.4 Purification of *H. pylori* HP0524Δ1

Attempts to overproduce the full-length form of HP0524 failed. However, overproduction of an N-terminally truncated protein lacking the first 170 residues (HP0524Δ1) was achieved with plasmid pHY524Δ1 (Table 2.2). Deletion of the first 170 residues of HP0524 removes three potential transmembrane helices predicted by the PHDhtm program (http://cubic.bioc.columbia.edu/predictprotein/). The primary difficulty in the purification of HP0524Δ1 was the solubilization of the protein. SDS complete cell extracts of induced *E. coli* (pHY524Δ1) cells contained large amounts of HP0524Δ1, but these remained insoluble under non-denaturing conditions when using Brij-58, Triton X-100, CHAPS, Zwittergent 3-16 and other detergents. Solubilization of HP0524Δ1 was achieved by the use of Zwittergent 3-14, a zwitterionic detergent containing a hydrophobic chain of 14 carbon atoms. These solubility properties were of great advantage for the purification of HP0524Δ1, yielding a crude protein extract of 50% purity; the extract was further purified by gel filtration (Table 4.4 and Figure 4.7).

However, the restricted solubility of HP0524Δ1, which imposed the presence of detergent and high salt concentration in all buffers used later, remained a serious disadvantage for the biochemical characterization of the protein.

Table 4.4. Purification of TraD and HP0524Δ1.

Protein	Fraction	Purification step	Protein [mg]	Yield [%][a]	Purity [%][b]
TraD	I	Crude extract	179	100	35
	II	Ni-NTA	34	23	42
HP0524Δ1	I	Crude extract	81	100	50
	II	Gel filtration	48	85	72

[a] Based upon TraD/HP0524Δ1 yield of fraction I
[b] Laser-densitometric evaluation of Coomassie-blue stained gels

4.4.5 Purification of R388 TrwBΔ1

R388 TrwBΔ1 is identical to TrwBΔN70, whose purification has been described (64), except that TrwBΔ1 carries an N-terminal His_6-tag. Purification of TrwBΔ1 was accomplished analogously to the purification of TraGΔ2. Consecutive Ni-NTA and phosphocellulose P11 chromatography yielded a TrwBΔ1 preparation of 97% purity (Figure 4.8and Table 4.5).

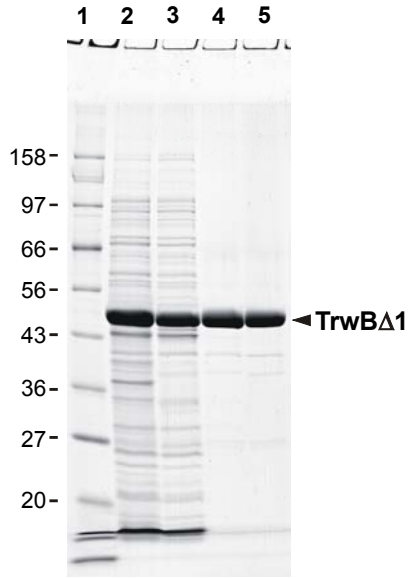

Figure 4.8. TrwBΔ1 was purified to homogeneity. Coomassie-Blue-stained gels of samples collected during the purification of TrwBΔ1, resolved by SDS-PAGE. Lane 1, marker proteins (sizes in kDa are indicated). Lane 2, SDS complete cell extract (20 µg). Lanes 3-5, samples of native protein extracts: 3, fraction I (17 µg); 4, fraction II (7 µg); 5, fraction III (7 µg).

Table 4.5. Purification of TrwBΔ1.

Fraction	Purification step	Total protein [mg]	Yield [%][a]	Purity [%][b]
I	Crude extract	715	100	44
II	Ni-NTA	264	81	97
III	Phosphocellulose P11	261	80	97

[a] Based upon TrwBΔ1 yield of fraction I
[b] Laser-densitometric evaluation of Coomassie-blue stained gels

4.5 The membrane anchor is responsible for oligomerization of TraG and TrwB

Cells grown at 37 °C or at 30 °C yielded equal amounts of overproduced full-length TraG, TraD or truncated HP0524, as evaluated on SDS-PAGE of SDS complete cell extracts (not shown). However, solubilization experiments under non-denaturing conditions revealed that the overproduced proteins were insoluble when cells had been grown at 37 °C, but could be solubilized when cells had been grown at 30 °C. This observation indicated that the overproduced TraG-like proteins might form insoluble aggregates in more rapidly growing cells.

In vitro formation of multimers or aggregates was deduced from several observations. Upon gel filtration, TraG and TraD eluted within the void volume of the column. The values for the elution volume of TraG remained unaltered when gel filtration was run with buffer containing 1M NaCl and 0.1 % Brij-58 or if samples of TraG were sonicated prior to gel filtration. Given that the gel filtration matrix used in these experiments has an exclusion limit of 1200 kDa, TraG and TraD probably form multimers or aggregates of at least 18 and 16 subunits, respectively (Figure 4.9 and Table 4.6).

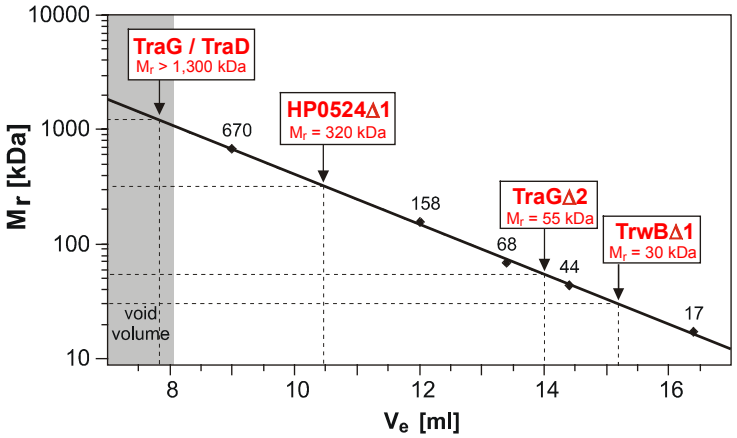

Figure 4.9. The molecular masses (M_r) of several TraG-like proteins and their derivatives were determined by gel filtration analysis. Elution volumes (V_e) of TraG, TraGΔ2, TraD and HP0524Δ1 were recorded and correlated to molecular masses. Protein standards (♦) in the 17-670 kDa range were used for calibration of the gel filtration column.

Table 4.6. Oligomeric states of TraG-like proteins and derivatives.

Protein	M_r of the monomer[a] [kDa]	M_r evaluated by SDS-PAGE [kDa]	M_r evaluated by gel filtration [kDa]	Deduced oligomeric state
TraG	70.8	71.2	> 1,300	> 18
TraD	82.2	81	> 1,300	> 16
HP0524Δ1	68	60	290-350	4-5
TraGΔ2	59.7	59.3	50 - 60	1
TrwBΔ1	49.6	47.3	27 - 33	1

[a] calculated from the predicted amino acid sequence

Glycerol gradient centrifugation of TraG and TraD resulted in very broad sedimentation profiles (Figure 4.11). Failure of both proteins to sediment as discrete bands indicated that TraG and TraD are polydisperse under the conditions applied. A molecular mass of approximately 320 kDa was calculated from the elution volume of HP0524Δ1, indicating that HP0524Δ1 forms multimers of 4 or 5 subunits. It is however difficult to draw conclusions from the latter observation because of the restricted solubility of HP0524Δ1. In contrast to full-length TraG, TraGΔ2 behaved as a monomer. Upon gel filtration, TraGΔ2 eluted in the 50-60 kDa range, which is in good accordance with its predicted monomer size (Table 4.6). Electron microscopy of TraG-DNA or TraGΔ2-DNA complexes provided additional evidence: the large protein aggregates seen with TraG-DNA complexes were not visible in TraGΔ2-DNA complexes (Figure 4.10). In these images, TraGΔ2 was invisible altogether. Probably, a single monomer of TraGΔ2 was too small to be detected by electron microscopy. The DNA binding properties of TraG and TraGΔ2 are discussed below (4.7).

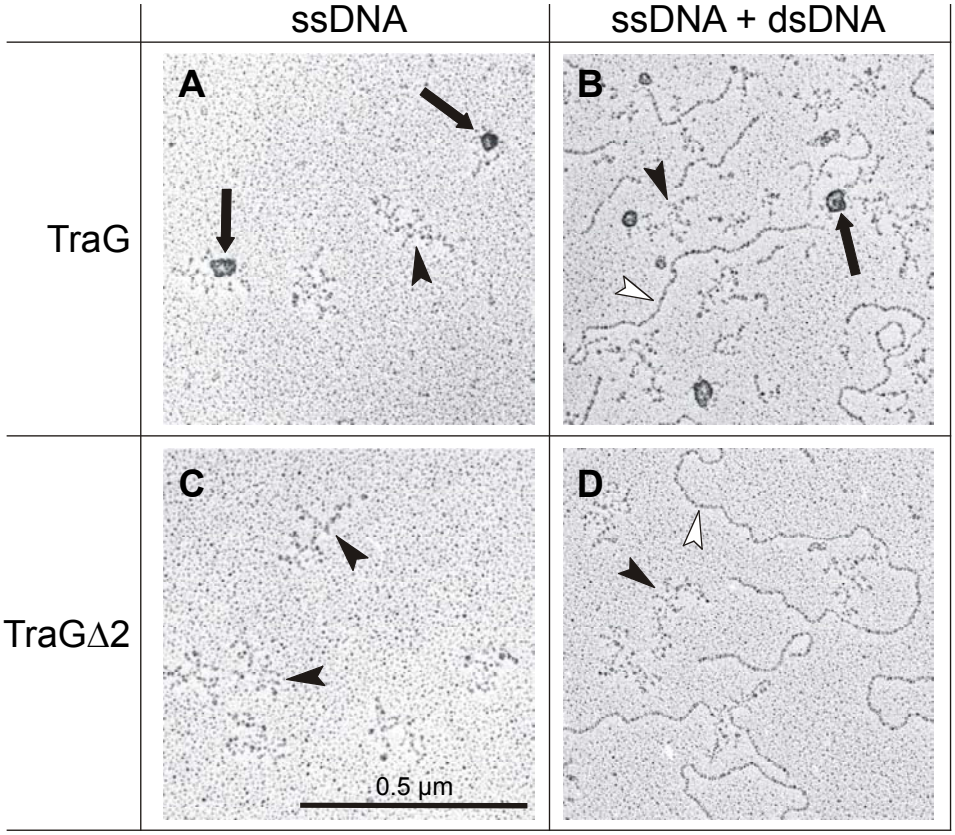

Figure 4.10. Removal of the membrane anchor of TraG suppresses its oligomerization. Electron microscopic images taken of full-length TraG (A and B) or TraGΔ2 preparations (C and D). The proteins were incubated with ssDNA alone (A and C) or with a 1:1 mixture of ssDNA and dsDNA (B and D) prior to fixation and adsorption to mica. ssDNA molecules are indicated by black arrowheads, dsDNA molecules are indicated by white arrowheads. Large protein oligomers that are bound to ssDNA (indicated by black arrows) were observed with TraG but were not found in TraGΔ2/DNA preparations.

Similarly to TraG, full-length or truncated forms of TrwB display a differential behavior regarding the oligomeric state: whereas solubilized full-length TrwB forms a mixture of monomers and hexamers (39), truncated derivatives TrwBΔN70 or TrwBΔ1 strictly behave as monomers (ref. 64 and Figure 4.9). Thus, removal of the membrane anchor of TraG and TrwB suppresses *in vitro* protein oligomerization or aggregation. It can be concluded that the membrane anchor of these TraG-like proteins is responsible for multimerization of the full-length proteins *in vitro* and possibly also *in vivo*.

4.6 TraG-like proteins do not hydrolyze nucleotides but bind to nucleoside di- and triphosphates

4.6.1 TraG-like proteins do not hydrolyze NTPs *in vitro*

TraG-like proteins contain two conserved motifs that resemble the nucleotide binding motifs of NTP hydrolases (NTPases). To verify this potential activity *in vitro*, purified proteins were incubated with γ-^{32}P-NTPs and the release of radioactive phosphate (P_i) or pyrophosphate (PP_i) was measured. ssDNA was added in control experiments in case it would be needed as a stimulator, as it is observed with helicases (74).

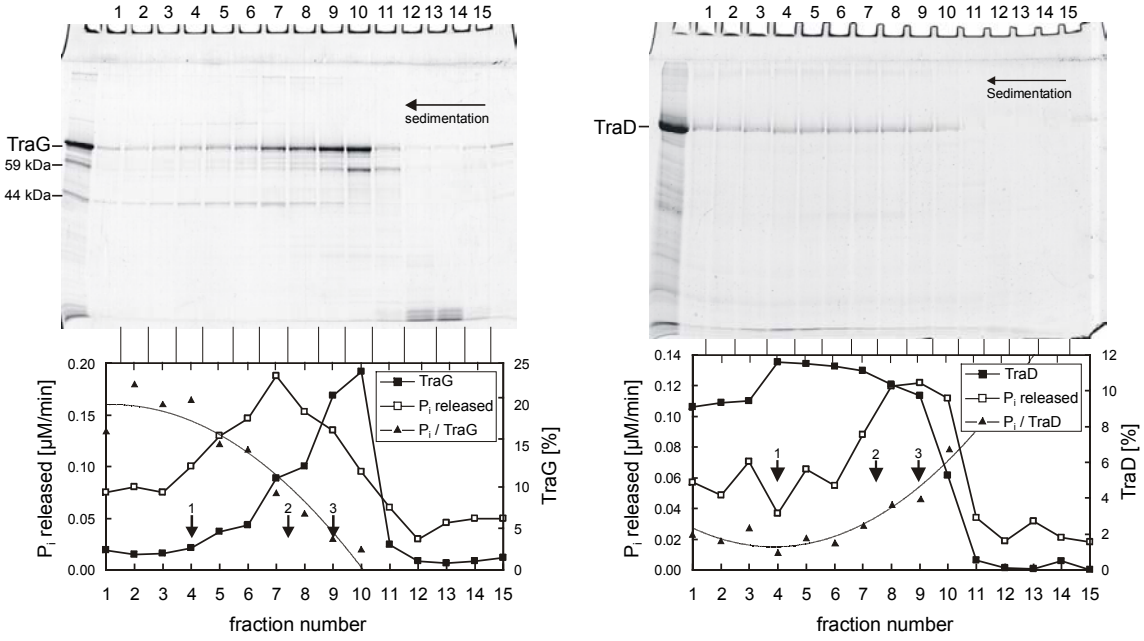

Figure 4.11. TraG and TraD preparations contained ATP hydrolyzing impurities that were removed by glycerol gradient centrifugation. Purified TraG or TraD was layered on a 15-35 % (w/v) linear glycerol gradient. Centrifugation was at 270,000 × g for 38 h. Aliquots of fractions were analyzed on a SDS-15% polyacrylamide gel (top) and were assayed for ATPase activity. The graph on the bottom shows the TraG or TraD content and the ATPase activity in each fraction. The ratio of ATPase activity to protein content (P_i / TraG or TraD) is also shown. Reference proteins 1-3 were centrifuged in a parallel experiment and sedimented as indicated by arrows. 1: aldolase, 158 kDa, $S_{20,w}$ = 7.8; 2: BSA, 67 kDa, $S_{20,w}$ = 4.4; 3: ovalbumin, 43.5 kDa, $S_{20,w}$ = 3.6. The very broad sedimentation profile of TraG and TraD indicate the presence of several oligomeric states of these proteins.

Full-length TraG and TraD were assayed for NTPase activity in a previous study (43). Here, ATP- and GTP-hydrolyzing activity, which could be stimulated by addition of ssDNA, was detected in TraG preparations (specific ATPase activity: 0.39 ± 0.05 µmol/min). However, the majority of this activity was separable from TraG by glycerol gradient centrifugation (Figure 4.11). The ATPase activity present in the collected fractions did not correlate with the amount of TraG (the plot P_i / TraG in Figure 4.11 is not a constant value), indicating that the NTPase activity present in the TraG preparation was conferred by impurities. Similarly, an ATPase activity that was also exerted by impurities was detected in the TraD preparation (activity: 3.5 ± 0.5 µmol/min; Figure 4.11, right).

In the present work, the potential ATPase activity of HP0524Δ1 and TraGΔ2 was verified. No ATPase activity was detectable in fractions collected from gel filtration of HP0524Δ1 (Figure 4.12), regardless of the presence or absence of ssDNA. ATPase activity assays with purified TraGΔ2 equally failed to detect hydrolase activity (not shown). Truncated TrwB has been reported to lack ATPase activity in an earlier study (64).

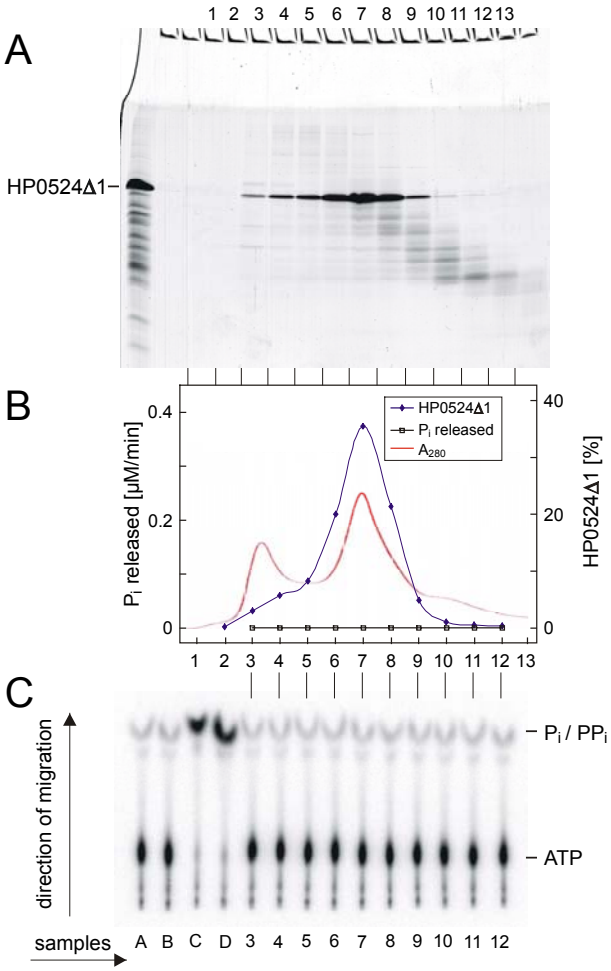

Figure 4.12. HP0524Δ1, purified by gel filtration, did not contain detectable ATPase activity. (A) Samples collected from gel filtration of HP0524Δ1 (crude extract) were analyzed on a SDS-15% polyacrylamide gel. **(B)** Diagram showing the 280 nm spectrum recorded during gel filtration (red curve), along with the HP0524Δ1 content (in % of total HP0524Δ1, blue curve) and the ATPase activity (expressed as time-dependent release of phosphate P_i, black curve) in each fraction. **(C)** ATPase activity assay. Fractions collected from gel filtration of HP0524Δ1 were incubated with γ-^{32}P-ATP in the presence of Mg^{2+} and ssDNA. Non-hydrolyzed ATP and released γ-phosphate (P_i) or pyrophosphate (PP_i) were separated by thin layer chromatography. A, proteins omitted; B, 5 pmol ATPase TraI (R1) plus 4 µl buffer H; C, 5 pmol TraI (R1); D, 5 pmol ATPase HP0525 (*H. pylori*) plus 4 µl buffer H; 3-12, 4 µl (2-80 pmol) of fractions 3-12 collected from gel filtration of HP0524Δ1 in buffer H. Sample 7 contained 60 pmol of HP0524Δ1.

In summary, each of the TraG-like proteins analyzed failed to hydrolyze nucleotides under the conditions applied. It can however not be excluded that TraG-like proteins may function as active NTPases *in vivo* under conditions that have yet to be determined. During the present study, a few of the many conditions that are theoretically possible were tested without success: neither ssDNA, nor RP4 proteins TraI or TrbE (75) were able to induce ATPase activity of TraG. Equally, Ca^{2+} and the VirB11-like protein HP0525 failed to stimulate the putatively latent ATPase activity of HP0524Δ1.

4.6.2 TraGΔ2 and TrwBΔ1 bind ATP and ADP.

TraGΔ2 and TrwBΔ1 were assayed for nucleotide binding by studying the binding of fluorescent ATP and ADP derivatives TNP-ATP and TNP-ADP. Binding of TNP-nucleotides causes an increase of fluorescence (enhanced fluorescence), a phenomenon that has been widely used to characterize the nucleotide binding ability of proteins (46). Fluorescence enhancement emerges from the changes in polarity in the near environment of the TNP-moiety upon binding (36, 63). As shown in Figure 4.13, addition of TraGΔ2 or TrwBΔ1 to TNP-ATP produced a significant fluorescence enhancement.

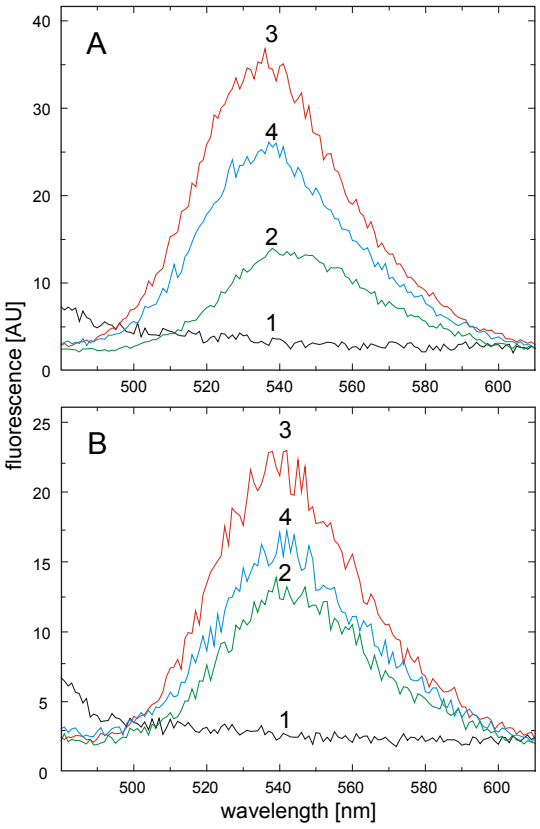

Figure 4.13. TraGΔ2 and TrwBΔ1 bind TNP-ATP. The fluorescent ATP analog TNP-ATP displayed enhanced fluorescence upon binding by TraGΔ2 **(A)** and TrwBΔ1 **(B)**. The fluorescence spectra 1-4 were taken from the following samples: 1, protein (7 µM); 2, TNP-ATP (50 µM); 3, protein (7µM) plus TNP-ATP (50 µM); 4, protein (7µM) plus TNP-ATP (50 µM) in the presence of ATP (10 mM). Fluorescence intensities are represented as arbitrary units (AU).

When TNP-ADP was used instead of TNP-ATP, the fluorescence was augmented to a similar extent. In both cases, fluorescence increase was coupled with a blue-shift of the fluorescence maximum from 542 nm to 528 nm, suggesting that the TNP-nucleotides bind to a hydrophobic region of the proteins (37). Competition experiments confirmed that nucleotide binding was specific, since addition of non-labeled nucleotide to TNP-nucleotide-protein complexes considerably reduced the fluorescence (Figure 4.13, curve 3 vs curve 4). In control experiments without protein, TNP-nucleotide fluorescence remained unchanged either by addition of the buffer contained in the used protein solutions, or by addition of non-labeled nucleotides (not shown).

Initial experiments to verify the ATP binding ability of full-length TraG failed. Although addition of TraG to TNP-ATP and TNP-ADP produced a significant fluorescence enhancement, the specificity of this effect could not be demonstrated: addition of non-labeled ATP or ADP did not revert the fluorescence increase caused by addition of TraG, i.e. TNP-nucleotide binding was not competed by nucleotides. A possible reason could be the presence of significant amounts of detergent (Brij-58) in TraG preparations. The observation that TraG stock solutions (in 50% glycerol) became opaque at –20°C, but became once again clear at 4°C was indeed indicative of this assumption. Moreover, fluorescence enhancement studies with Brij-58 confirmed that addition of the detergent produced a fluorescence enhancement of TNP-nucleotides.

4.6.3 The dissociation constants (K_d) for nucleotide binding of TraGΔ2 and TrwBΔ1 were determined to be in the 10^{-1} mM range

Dissociation constants (K_d) for the binding of TNP-ATP and TNP-ADP were determined by titration of 7 μM solutions of TraGΔ2 and TrwBΔ1 with TNP-nucleotides, until saturation was observed (shown for TraGΔ2 in Figure 4.14, A and B). Saturation of the proteins by TNP-nucleotides is well described by a function that relates fluorescence enhancement (ΔF) with total TNP-nucleotide concentration, total protein concentration, K_d and the maximum fluorescence enhancement (Eq. 5 in chapter 3.13). Computational fitting of Eq. 5 to the experimentally determined values delivered the K_d values for TNP-ATP and TNP-ADP binding of TraGΔ2 and TrwBΔ1, which were in the 4-5 μM range (Table 4).

Binding of TNP-nucleotides has often been observed to be stronger than binding of the non-labeled nucleotides. This can be attributed to hydrophobic interactions between the TNP-moiety and the protein that should additionally stabilize complexes, provided that

nucleotide binding itself is not disturbed. In order to determine the true dissociation constants of ATP and ADP, the displacement of bound TNP-nucleotides by non-labeled nucleotides was quantified. Titration of TNP-nucleotide-saturated TraGΔ2 and TrwBΔ1 with excess of the respective nucleotide caused progressive decrease of fluorescence (shown for TraGΔ2 in Figure 4.14, C and D).

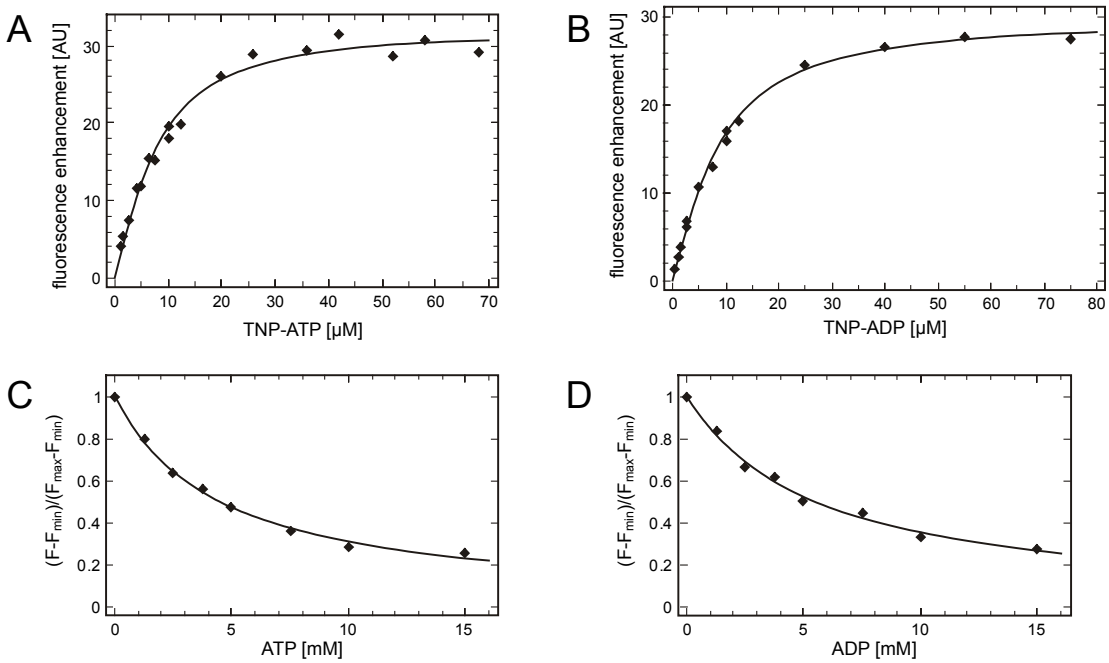

Figure 4.14. Determination of the dissociation constants (K_d) for ATP- and ADP-binding of TraGΔ2. (A, B) Saturation curves obtained by titration of TraGΔ2 (7 µM) with TNP-ATP and TNP-ADP. Binding of TNP-nucleotides was monitored by measuring the fluorescence enhancement, i.e. the difference between intrinsic TNP-nucleotide fluorescence and fluorescence of bound TNP-nucleotides. The curves represent the best fit obtained with Eq. 5 (3.13), which delivered the K_d values for TNP-nucleotide binding. **(C, D)** Displacement of bound TNP-nucleotides by unlabeled nucleotides, causing a decrease in fluorescence. C, ATP was added to a mixture of TraGΔ2 (7 µM) and TNP-ATP (50 µM). D, ADP was added to a mixture of TraGΔ2 (7 µM) and TNP-ADP (70 µM). The curves were calculated using Eq. 6 that contains constants for minimal and maximal fluorescence (F_{min} and F_{max}). The derived K_d values are listed in Table 4.7.

Computational fitting of Eq. 6 (3.13) to the data delivered the concentration of ATP/ADP that caused 50% dissociation of TNP-nucleotide-protein complex (I_{50}). In combination with the K_d of TNP-nucleotide binding that was determined before, this provided the K_d for ATP/ADP binding (Table 4). Nucleotide binding was hereby determined to be in the range of K_d = 0.3-0.4 mM for TraGΔ2 and was somewhat stronger in case of TrwBΔ1 (K_d = 0.1-0.2 mM). Thus, binding of non-labeled nucleotides was significantly lower than binding of the fluorescent TNP-derivatives (30 to 40 –fold lower for TrwBΔ1 and up to 80-fold lower in case of TraGΔ2).

Table 4.7. K_d values for binding of ATP, ADP and TNP-nucleotides.

Protein	$K_d^{TNP\text{-}ATP}$ [μM]	$K_d^{TNP\text{-}ADP}$ [μM]	K_d^{ATP} [mM]	K_d^{ADP} [mM]
TraGΔ2	4.1	5.1	0.34	0.37
TrwBΔ1	4.5	3.9	0.13	0.17
TraGΔ2K187T	6.0	7.2	0.81	1.64

4.6.4 Mutation in the putative nucleotide binding site of TraG (TraGΔ2K187T) causes reduction of its ATP- and ADP-binding ability.

Nucleotide binding of derivative TraGΔ2K187T was determined as before, by monitoring the fluorescence enhancement of TNP-ATP and TNP-ADP. Binding of TNP-nucleotides was only slightly weaker than seen with TraGΔ2. Evaluation of the saturation curves for binding of TNP-ATP and TNP-ADP to TraGΔ2K187T resulted in dissociation constants of $K_d^{TNP\text{-}ATP}$ = 6.0 μM and $K_d^{TNP\text{-}ADP}$ = 7.2 μM. However, displacement experiments with unlabelled nucleotides revealed that the binding ability of mutant TraGΔ2K187T for ATP and ADP was considerably reduced (Figure 4.15). Dissociation constants of K_d^{ATP} = 0.81 mM and K_d^{ADP} = 1.64 mM indicated a 2.4 fold and 4.5 fold decrease in binding affinity for ATP and ADP, respectively.

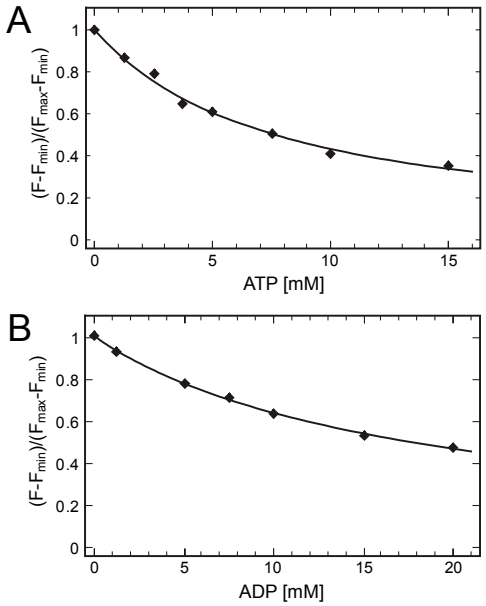

Figure 4.15. TraGΔ2K187T point mutation derivative has a decreased nucleotide binding ability. The K_d values for ATP- and ADP-binding of TraGΔ2K187T were determined by monitoring the displacement of protein-bound TNP-nucleotides by unlabeled nucleotides. Displacement manifested itself as a decrease in fluorescence. **(A)** ATP was added to a mixture of TraGΔ2K187T (7μM) and TNP-ATP (50 μM). **(B)** ADP was added to a mixture of TraGΔ2K187T (7μM) and TNP-ADP (70 μM). The curves were calculated using the best fit to Eq. 6 (3.13), yielding dissociation constants for ATP- and ADP binding.

4.6.5 TNP-ATP-binding of TraGΔ2 and TrwBΔ1 is inhibited in the presence of Mg^{2+} and DNA and is competed by other nucleotides.

In analogy to the competition experiments performed with excess ATP (see above), other nucleotides and nucleotide derivatives were assayed for their ability to displace TNP-ATP. Additionally, the effect of inorganic salts and DNA was tested (Figure 4.16). For both TraGΔ2 and TrwBΔ1, Mg^{2+} had the largest effect (80% reduction of ΔF). This was also the case for displacement of protein-bound TNP-ADP (not shown). The inhibition constant for Mg^{2+}-inhibition of TraGΔ2/TNP-ATP-binding was determined to be K_i = 82 µM. DNA, especially single-stranded DNA, was also a strong inhibitor for TNP-ATP-binding of TrwBΔ1, but was a much weaker inhibitor in case of TraGΔ2.

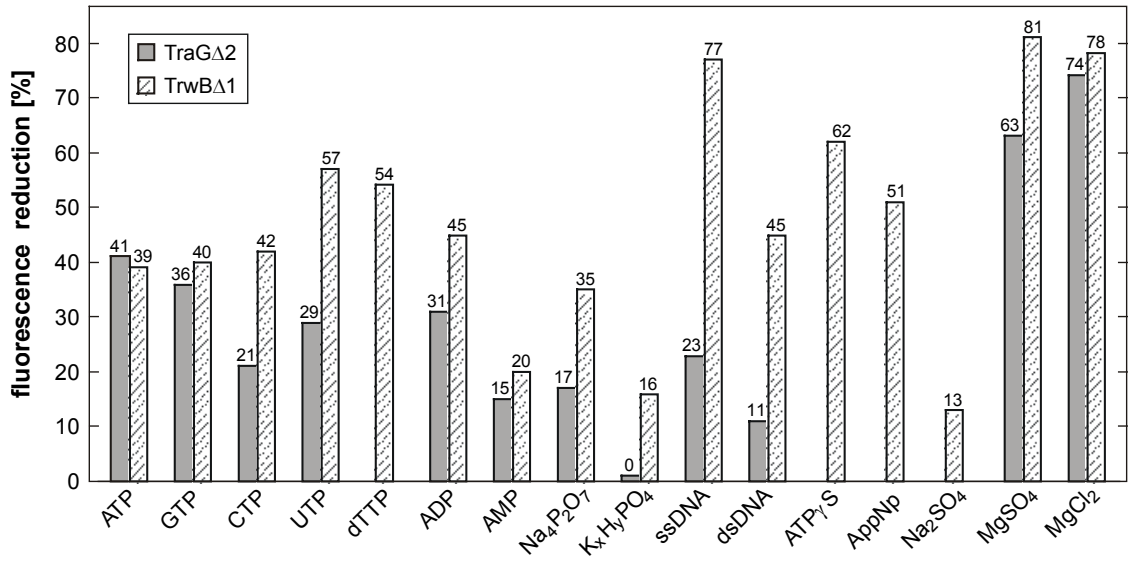

Figure 4.16. Displacement of bound TNP-ATP by other nucleotides, DNA and inorganic salts. Fluorescence of TNP-ATP/protein-mixtures was measured before and after addition of the indicated compounds. The percentage of fluorescence reduction was set as a measure for the displacement of bound TNP-ATP, i.e. as a measure for competition for the binding site or inhibition of nucleotide-binding. Concentrations were as follows: TraGΔ2 or TrwBΔ1 (10 µM); TNP-ATP (50 µM); nucleotides, $K_xH_yPO_4$, AppNp, Na_2SO_4, $MgSO_4$, $MgCl_2$ (5 mM); $Na_4P_2O_7$, ATPγS (2.5 mM); ssDNA (18 nM); dsDNA (15nM).

All nucleotides and nucleotide derivatives tested were able to compete for TNP-ATP to a certain extent. In case of TraGΔ2, ATP itself was the best natural competitor for TNP-ATP, whereas UTP and dTTP were most effective with TrwBΔ1. These observations indicated that purine or pyrimidine moieties of nucleotides did not particularly add to the specificity of nucleotide binding of TraGΔ2 or TrwBΔ1. Synthetic ATP analogues ATPγS and AppNp were able to displace TNP-ATP to a higher extent than ATP. ADP was a good competitor for both proteins, whereas competition by AMP was poor. Similarly, pyrophosphate (PP_i) was a much better competitor than phosphate, although

at an overall lower rate than ADP. Thus, there seems to be binding specificity for at least the diphosphate moiety of NTPs or NDPs, whereas purine or pyrimidine moieties are more or less equally well bound and merely add to the strength of binding.

4.7 TraG-like proteins bind to DNA *via* the cytoplasmic domain

4.7.1 TraG, TraD and HP0524Δ1 bind to DNA with varying specificity for ss- or ds-DNA

TraG, TraD and HP0524Δ1 were tested for DNA binding ability and possible specificity for *oriT* sequences. Fragment retardation (fragment shift) experiments on non-denaturing gels revealed that all three proteins possess double-stranded DNA (dsDNA) binding ability (Figure 4.17 and Figure 4.18).

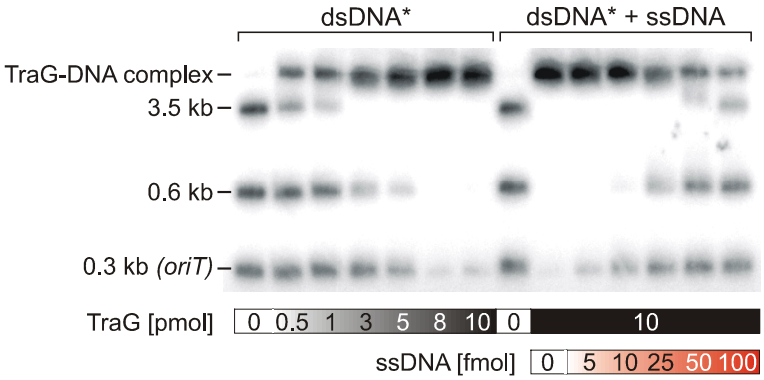

Figure 4.17. RP4 TraG binds to both dsDNA and ssDNA with preference for ssDNA. (Left) ^{32}P-labeled (*) dsDNA fragments (75 fmol) were incubated with increasing amounts of TraG and were electrophoresed on a non-denaturing polyacrylamide gel. Protein-DNA complexes were retained in the gel slots. The 0.3 kb DNA fragments contains the core sequence of RP4 *oriT*, the other DNA fragments originate from the vector pBR329. (Right) Increasing amounts of ssDNA were added as competitor to a previously incubated dsDNA/TraG mixture. dsDNA was seen to be released from TraG in the presence of small amounts of ssDNA.

The experiments showed that addition of increasing amounts of protein to radiolabeled dsDNA fragments caused a mobility-shift of the DNA fragments upon gel electrophoresis. This protein-induced fragment retardation was indicative of the formation of dsDNA-protein complexes. The 3.5 kb vector DNA fragment was bound to 100% in the presence of 3 pmol TraG, whereas 5 pmol HP0524 and 100 pmol TraD was needed for reaching the same amount of bound fragments. Thus, the DNA binding affinity of TraG was highest, if compared to HP0524Δ1 and TraD with intermediate and weak binding affinity, respectively. The fact that the largest, 3.5 kb vector DNA fragment was bound preferentially, followed by the 0.6 kb and the 0.3 kb DNA fragments, indicated that the DNA was bound without sequence specificity and that

multiple binding sites are present on the larger fragments. Thus, TraG had no binding preference for RP4 *oriT*. Likewise, TraD did not preferentially bind to F *oriT*-containing DNA fragments (data not shown).

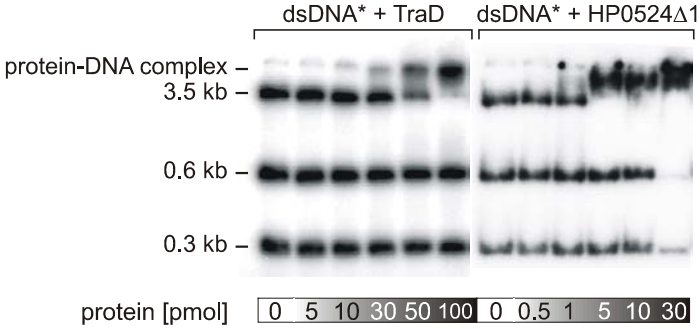

Figure 4.18 TraD and HP0524Δ1 bind to dsDNA. ^{32}P-labeled (*) dsDNA fragments were incubated with the indicated amounts of TraD or HP0524Δ1 and electrophoresed on a non-denaturing polyacrylamide gel. Protein-DNA complexes were retained in the gel slots.

In competition assays, the addition of unlabeled ssDNA to a previously incubated protein-dsDNA mixture showed that ssDNA is the preferred binding substrate for TraG and TraD (as shown for TraG in Figure 4.17). In contrast, HP0524Δ1-dsDNA complexes remained intact after addition of competitor ssDNA (not shown), indicating that dsDNA is the preferred substrate for HP0524Δ1. Complexes of TraG and TraD with dsDNA or ssDNA were also visualized by electron microscopy. When a mixture of equal amounts of ssDNA and dsDNA was incubated with the proteins, complex formation was seen to occur only with ssDNA (shown for TraG in Figure 4.10). In these images, TraG and TraD were observed to form oligomers or aggregates that are complexed to the DNA.

4.7.2 Removal of the membrane anchor of TraG or point mutation in the putative P-loop motif does not affect the DNA binding ability of TraG

The DNA binding ability of TraG remained unaffected by the removal of the membrane anchor, as was demonstrated in fragment shift experiments with TraGΔ2 (Figure 4.19). Comparably high DNA binding affinity was also found for the mutant protein TraGΔ2K187T (not shown). Thus, DNA binding does neither require the N-terminal membrane anchor, nor the conserved residue K187 of the putative P-loop structure (Walker A motif). Consistently with the studies with full-length TraG, no specificity for *oriT* containing fragments was detected for TraGΔ2 or TraGΔ2K187T.

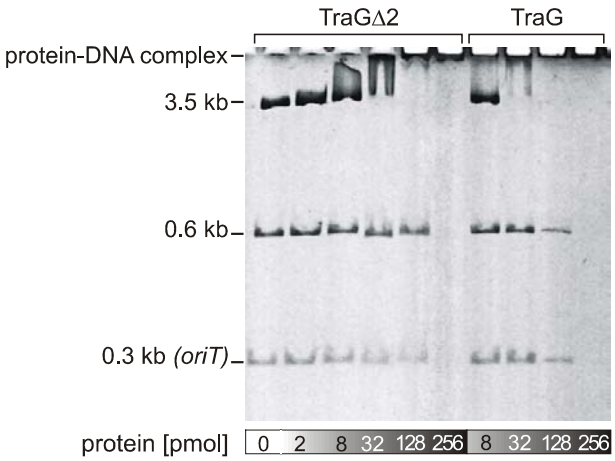

Figure 4.19. The cytoplasmic domain of TraG binds DNA with the same affinity as full-length TraG. The indicated amounts of TraGΔ2 and TraG were incubated with dsDNA fragments (0.25 pmol each) and electrophoresed on a non-denaturing polyacrylamide gel. DNA was visualized by ethidium bromide staining. Protein-DNA complexes were retained in the gel slots. As before, no binding preference was observed for the *oriT* containing 0.3 kb fragment.

4.7.3 Dissociation constants for dsDNA-binding of TraGΔ2 and TrwBΔ1 were determined.

The DNA-binding activity was standardized in order to determine dissociation constants that can be compared between different proteins or protein derivatives. Fragment shift experiments were carried out with a single 0.8 kbp DNA fragment isolated from pBR329 (Figure 4.20). As before, protein-dsDNA complexes did not produce a discrete band but accumulated in the wells of the gel. In these complexes, multiple protein molecules may bind to the DNA, up to a saturation level. DNA fragments with intermediate mobility are visible as a smear in the gel. Such fragments are probably not fully occupied with bound proteins and are therefore more mobile than protein-saturated fragments. The apparent dissociation constants (K_d^{app}) of TraGΔ2 and TrwBΔ1 for binding of the 0.8 kb fragment were determined as K_d^{app} = 75 nM and K_d^{app} = 24 nM, respectively. Thus, the dsDNA-binding affinity of TrwBΔ1 is three times higher than the one measured for TraGΔ2.

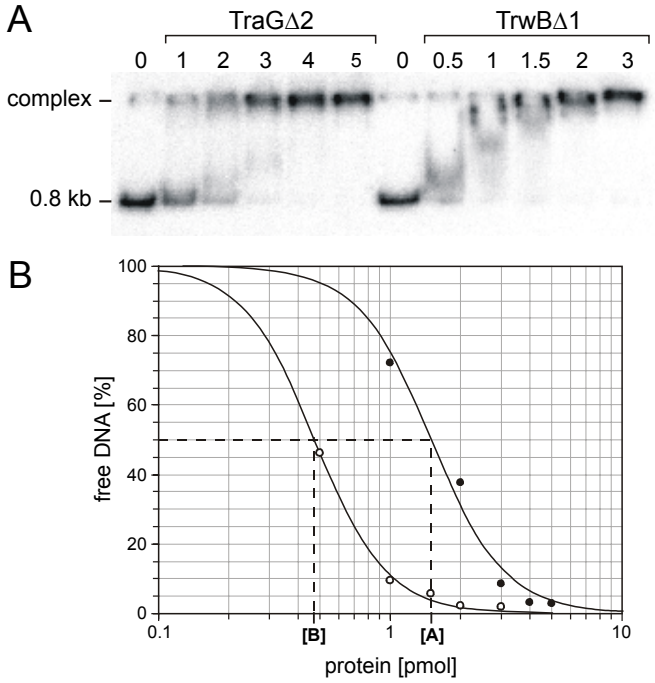

Figure 4.20. dsDNA-binding activity of TraGΔ2 and TrwBΔ1. (A) Fragment shift experiment of TraGΔ2 and TrwBΔ1 incubated with a 0.8 kb ^{32}P-labeled dsDNA fragment. Increasing amounts of protein (indicated in pmol) were added to 36 fmol of the dsDNA fragment. **(B)** Bjerrum plot of free DNA as a function of protein concentration. Complex formation with TraGΔ2 (filled circles) or with TrwBΔ1 (open circles) was determined by quantifying the fraction of free DNA. The amount of protein necessary to bind half of the DNA was calculated using the Hill-type equation that describes a symmetrical hyperbola ([A] = 1.5 pmol TraGΔ2 and [B] = 0.47 pmol TrwBΔ1).

4.7.4 dsDNA binding of TraGΔ2 and TrwBΔ1 is competed by ssDNA and is weakly inhibited by the presence of Mg^{2+} and nucleotides.

Similarly to the fragment shift experiments performed with full-length TraG and TraD (4.7.1), dsDNA binding of truncated proteins TraGΔ2 and TrwBΔ1 was competed by ssDNA (Figure 4.21). Submolar ratios of ssDNA were sufficient to chase 50% of bound dsDNA, indicating that ssDNA was preferentially bound. The molar ratios (expressed in bases) necessary for 50% displacement were determined to be 1:5.4 (TraGΔ2) and 1:8.7 (TrwBΔ1). Since nucleotide binding of TraG and TrwB was observed to be inhibited by the presence of DNA (see above), it was verified whether nucleotides could reversibly inhibit DNA-binding. DNA fragment shifts were thus performed in the presence or absence of ATP and ADP. Additionally, the effect of Mg^{2+} was tested (Figure 4.21, lanes 6-8 and 14-16).

With TraGΔ2, inhibition was significant in case of Mg^{2+} (24% complex resolution) but was very low in case of ATP and ADP. With TrwBΔ1, ATP was the strongest inhibitor (37% complex resolution), followed by ADP and Mg^{2+} (13% and 16% complex resolution, respectively). Thus, inhibition by nucleotides was only observed for

TrwBΔ1, whereas inhibition by Mg^{2+} applied to both proteins, although at a much lower degree than had been observed in case of nucleotide-binding.

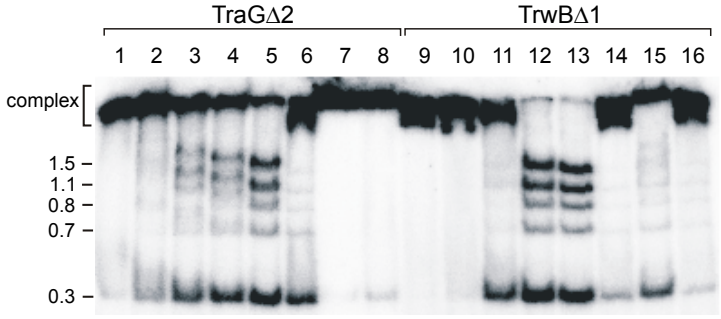

Figure 4.21. Displacement of protein-bound dsDNA by single-stranded DNA (ssDNA), Mg^{2+} or nucleotides. ^{32}P-labeled dsDNA fragments of pJF143 (75 fmol each, sizes indicated in kbp) were incubated with TraGΔ2 (10 pmol, lane 1-8) or TrwBΔ1 (3 pmol, lane 9-16) and then supplemented with competitor/inhibitor. Complexes were separated from free DNA by electrophoresis on a non-denaturing polyacrylamide gel. Lane 1 and 9, protein plus dsDNA; Lane 2-5, ssDNA added (6, 9, 12 and 18 fmol, respectively); Lane 10-13, ssDNA added (3, 6, 9 and 18 fmol, respectively); Lane 6 and 14, $MgCl_2$ (10 mM) added; Lane 7 and 15, ATP (10 mM) added; Lane 8 and 16, ADP (10 mM) added.

4.8 TraG oligomers interact with the relaxase TraI of RP4

4.8.1 TraG binds tightly and specifically to TraI

Indications for a putative interaction between TraG-like proteins and components of the relaxosome have been reported earlier. To obtain clear evidence for this hypothesis, the interaction between purified RP4 proteins TraG and TraI was studied *in vitro* by using the surface plasmon resonance (SPR) technology (BIACORE®). SPR is a state-of-the-art technique for *in vitro* detection and analysis of protein-protein interactions. It enables real-time monitoring of a binding reaction between an immobilized receptor and an added ligand.

For detection of the putative TraG-TraI interaction, purified TraI protein was immobilized to a sensor chip surface of a flow cell and BSA was immobilized in a reference unit. When TraG was injected into the flow cells, tight binding to TraI was observed, while BSA and the bald chip surface remained unbound (A in Figure 4.22). This demonstrated that TraG specifically binds to TraI. The association rate constant was determined to be $k_a = 1.3 \times 10^5\ M^{-1}s^{-1}$ (B in Figure 4.22). Dissociation of the TraG-TraI complex was only observed under harsh conditions (i.e. 0.01 % SDS or 0.2 M Na_2CO_3/pH 11.3).

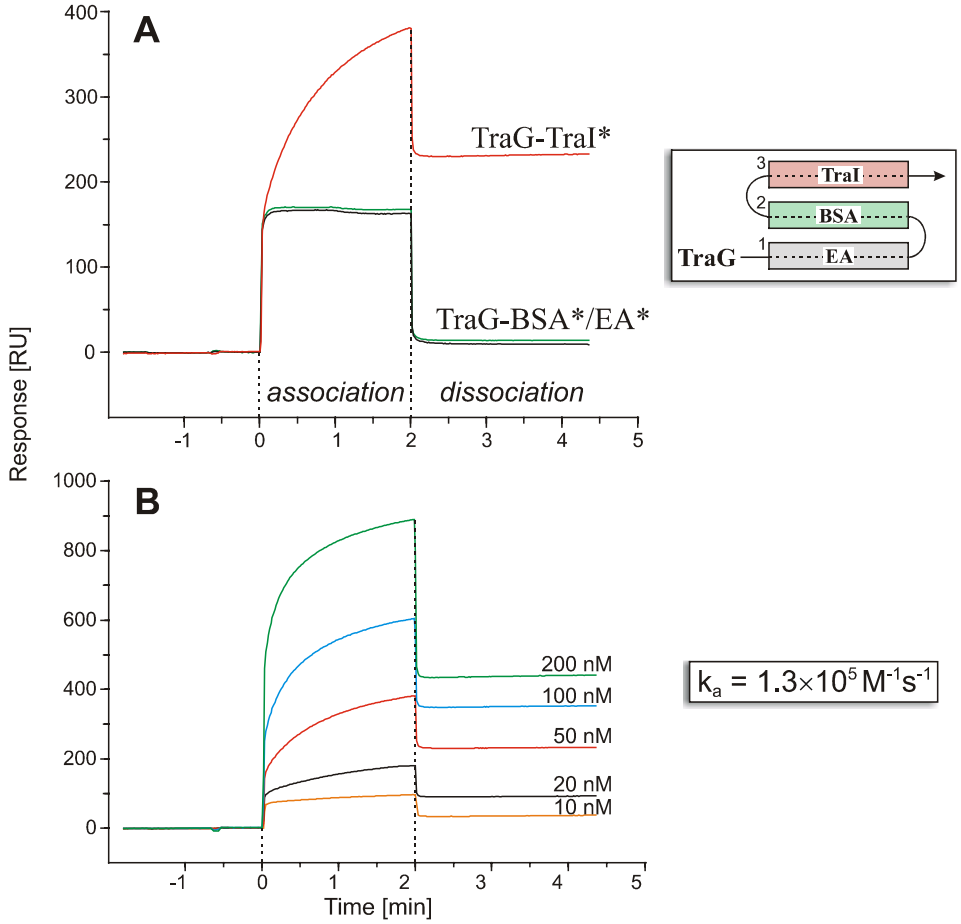

Figure 4.22. TraG binds tightly and specifically to the relaxase TraI of RP4. Complex formation between TraG and TraI was monitored in real time by surface plasmon resonance (SPR) analysis. TraI was covalently attached to the sensor chip by amide coupling (TraI*). Immobilized ethanolamine (EA*) and BSA (BSA*) in flow cells 1 and 2, respectively, served as a control for specificity. Upon injection, TraG protein solution flowed through flow cells 1, 2 and 3 successively (see scheme next to graph A). **(A)** Specific binding of 30 nM TraG to immobilized TraI expressed in resonance units per second (RU/s). The "binding curves" of non-specific interaction with EA and BSA are displayed for comparison. At injection start (0 min) and end (2 min), the abrupt change in RU in all flow cells is due to the contribution of "bulk solution" on the surface layer of the sensor chip. **(B)** Binding of TraG to immobilized TraI at five different ligand concentrations. The association rate constant (k_a) was determined by using the Langmuir binding model for 1:1 interaction between analyte and ligand.

4.8.2 The membrane anchor of TraG is essential for interaction with TraI

In addition to full-length TraG, derivatives TraGK187T and truncated derivatives TraGΔ2 and TraGΔ2K187T were assayed for their ability to interact with TraI. Real-time interactions with TraG derivatives were monitored on chip surfaces containing immobilized TraI, TraGΔ2 and BSA as a reference (Figure 4.23).

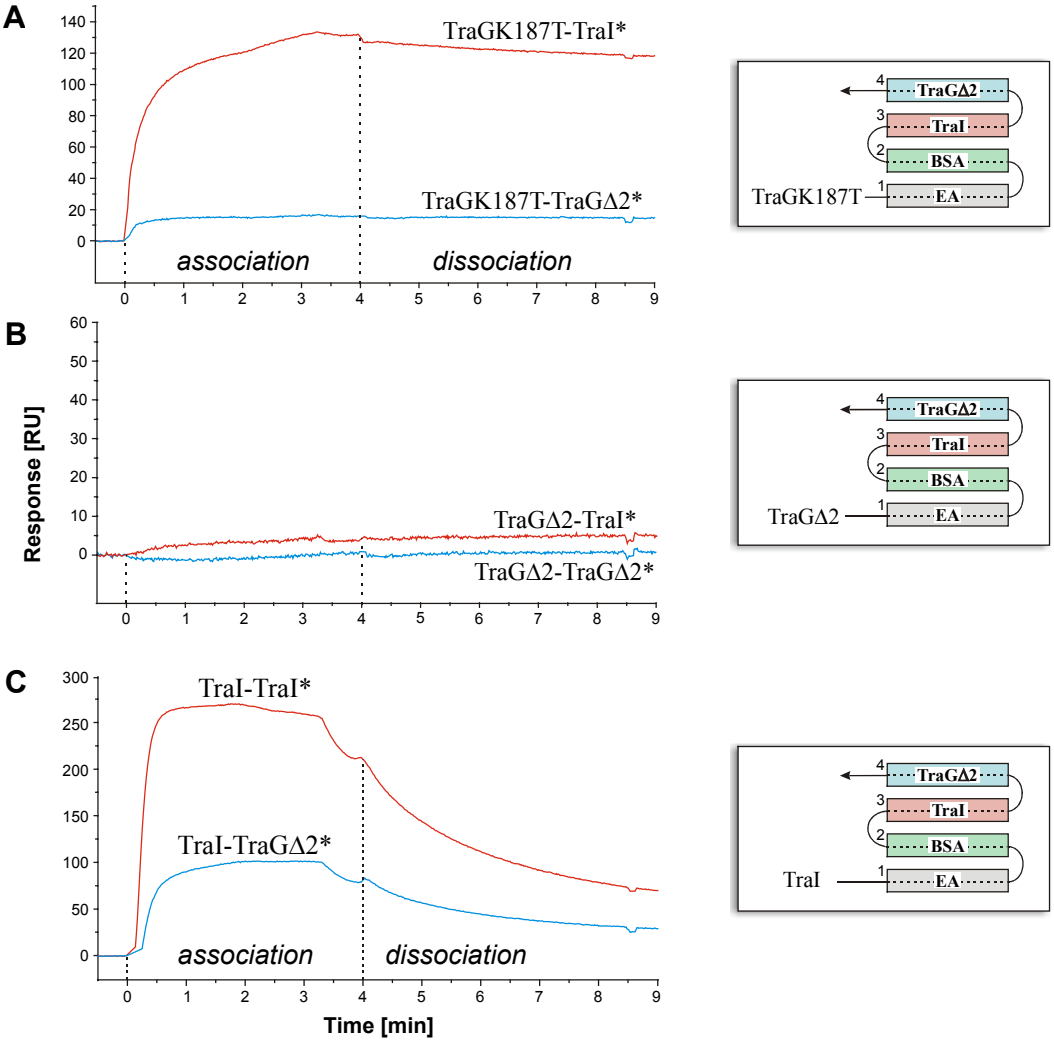

Figure 4.23. Interactions between TraG derivatives and relaxase TraI. The binding affinity between TraGK187T, TraGΔ2 and TraI, as well as intermolecular self-interactions were measured by SPR analysis on sensor chip surfaces. The sensor chip contained immobilized TraI (TraI*, red) and immobilized TraGΔ2 (TraGΔ2*, blue). BSA (green) and ethanolamine (grey) in flow cells 1 and 2 served as a reference. Real-time interactions with the immobilized proteins were monitored by injecting 100 nM solutions of TraGK187T (A), TraGΔ2 (B) or TraI (C) through all flow cells for four minutes. Signals were corrected for non-specific interactions by subtracting the curve measured for BSA interaction from each curve.

TraGK187T interacted with TraI to the same extent as observed for wild type TraG (panel A, red curve), indicating that conserved residue K187 of nucleotide binding motif A is not required for interaction with TraI. As before, the association to TraI was rapid ($k_a \approx 10^5\ M^{-1}$). Dissociation of the TraGK187T-TraI complex was negligibly slow ($k_d \approx 10^{-4}\ s^{-1}$). In contrast to TraG and TraGK187T, the truncated TraG derivatives, TraGΔ2 and TraGΔ2K187T did not interact with TraI. In these experiments, the response unit signals stayed indifferently low (shown for TraGΔ2 in Figure 4.23, panel B). Thus, the membrane anchor, but not the nucleotide binding motif of TraG is required for TraG-TraI interaction.

A different aspect of the TraG-TraI interaction arose when the reverse binding reaction was studied, i.e. when free TraI was tested for interaction with immobilized TraGΔ2. In this case, TraI was observed interact with TraGΔ2 (blue curve in Figure 4.23, panel C). Association and dissociation were slightly faster than before ($k_a \approx 10^6$ M^{-1} and $k_d \approx 10^{-3}$ s^{-1}). A plausible model explaining the differential observations for TraGΔ2-TraI interactions is presented in the discussion (page 69ff.). In addition to the TraI-TraGΔ2 interactions, intermolecular self-interactions were detected for TraI (red curve in Figure 4.23, panel C). Computational fitting provided k_a and k_d values ($k_a \approx 1.8 \times 10^6$ M^{-1} and $k_d \approx 2.5 \times 10^{-3}$ s^{-1}). This finding gives additional evidence for the previously postulated dimerization of TraI (72).

Interaction of full-length TraG with TraGΔ2 was hardly detectable (shown for TraGK187T in Figure 4.23, panel A, blue curve). Also, TraGΔ2 self-interactions were absent (blue curve in Figure 4.23, B). These data are in line with the previous observation, that, unlike full-length TraG, TraGΔ2 is a monomer (gel filtration and electron microscopy, see 4.5). Thus, the membrane anchor of TraG is required for both TraI interaction and self-interaction (oligomerization).